October 5, 2016

Docket: PROJ0769

U.S. Nuclear Regulatory Commission
ATTN: Document Control Desk
One White Flint North
11555 Rockville Pike
Rockville, MD 20852-2738

SUBJECT: NuScale Power, LLC Submittal of Topical Report TR-0116-21012, "NuScale Power Critical Heat Flux Correlation NSP2," Revision 0 (NRC Project No. 0769)

NuScale hereby submits Topical Report TR-0116-21012, "NuScale Power Critical Heat Flux Correlation NSP2," Revision 0. The purpose of this submittal is to request that the NRC review and approve the NSP2 critical heat flux correlation for use in VIPRE-01, within its range of applicability, along with its associated limit of 1.17, for the NuScale Design Certification Application and safety analysis of the NuScale Power Module with NuFuel-HTP2™ fuel. NuScale respectfully requests that the acceptance review be completed in 60 days from the date of transmittal.

Enclosure 1 contains the proprietary version of the report entitled "NuScale Power Critical Heat Flux Correlation NSP2." NuScale requests that this enclosure be withheld from public disclosure pursuant to 10 CFR § 2.390. The enclosed affidavit (Enclosure 3) supports this request. Enclosure 1 has also been determined to contain Export Controlled Information. This information must be protected from disclosure per the requirements of 10 CFR § 810. Enclosure 2 contains the nonproprietary version of the report entitled "NuScale Power Critical Heat Flux Correlation NSP2."

The enclosed affidavit (Enclosure 4) pertains to the AREVA proprietary information to be withheld from the public. AREVA proprietary information is denoted in the enclosures by straight brackets (i.e., "[ ]").

This letter makes no regulatory commitments and no revisions to any existing regulatory commitments.

Please feel free to contact Jennie Wike at 541-360-0539 or at jwike@nuscalepower.com if you have any questions.

Sincerely,

Thomas A. Bergman
Vice President, Regulatory Affairs
NuScale Power, LLC

Distribution: Frank Akstulewicz, NRC, TWFN-6C20
Greg Cranston, NRC, TWFN-6E7
Omid Tabatabai, NRC, TWFN-6E7
Mark Tonacci, NRC, TWFN-6E7

Enclosure 1: "NuScale Power Critical Heat Flux Correlation NSP2," TR-0116-21012-P, Revision 0, proprietary version
Enclosure 2: "NuScale Power Critical Heat Flux Correlation NSP2," TR-0116-21012-NP, Revision 0, nonproprietary version
Enclosure 3: NuScale Affidavit, AF-0916-51388
Enclosure 4: AREVA Affidavit

Enclosure 1:

"NuScale Power Critical Heat Flux Correlation NSP2," TR-0116-21012-P, Revision 0, proprietary version

NuScale Power, LLC
1100 NE Circle Blvd., Suite 200 Corvallis, Oregon 97330 Office 541.360-0500 Fax 541.207.3928
www.nuscalepower.com

Enclosure 2:

"NuScale Power Critical Heat Flux Correlation NSP2," TR-0116-21012-NP, Revision 0, nonproprietary version

NuScale Power Critical Heat Flux Correlation NSP2

October 2016

Revision 0

Docket: PROJ0769

NuScale Power, LLC

1100 NE Circle Blvd., Suite 200

Corvallis, Oregon 97330

www.nuscalepower.com

NuScale Nonproprietary

Department of Energy Acknowledgement and Disclaimer

This material is based upon work supported by the Department of Energy under Award Number DE-NE0000633.

CONTENTS

TABLES

FIGURES

Abstract

The purpose of this report is to provide the bases for Nuclear Regulatory Commission approval to use the NSP2 critical heat flux (CHF) correlation in VIPRE-01, within its range of applicability in Table 7-2, along with its associated correlation limit of 1.17, for the NuScale Power, LLC, Design Certification Application (DCA) and safety analysis of the NuScale Power Module (NPM) with NuFuel-HTP2™ fuel. This correlation conforms to acceptance criteria given by the NuScale Design-Specific Review Standard (DSRS), Section 4.4 (Reference 8.1.3), and the requirements of 10 CFR 50, Appendix A, General Design Criterion (GDC) 10.

This report describes the development of the NuScale NSP2 CHF correlation for the NPM. The figure of merit for preventing the occurrence of CHF in the NPM is critical heat flux ratio (CHFR), rather than departure from nucleate boiling ratio that is traditionally used for pressurized water reactor (PWR) applications.

The CHF tests for a preliminary prototypical fuel assembly design for NuScale, performed at Stern Laboratories, Inc. in Ontario, Canada, are used to develop a base CHF correlation. This preliminary prototypical assembly design utilizes a different spacer grid design than that used on the NuFuel-HTP2™ fuel design referenced in the NuScale DCA. A set of CHF data from AREVA testing of an assembly design that includes the HMP™ spacer grids used in the NuFuel-HTP2™ design is used to develop an “NSPX factor” for the base correlation that conservatively predicts NuFuel-HTP2™ CHF performance. The NSP2 CHF correlation is based on the combination of the base CHF correlation and this NSPX factor and is validated with data from design specific CHF testing for the NuFuel-HTP2™ fuel design performed at AREVA’s Karlstein, Germany thermal-hydraulic (KATHY) test facility. This report describes the tests, test facilities, statistical methods, base CHF correlation development, NSPX factor development, and final validation.

Executive Summary

The purpose of this report is to provide the bases for Nuclear Regulatory Commission approval to use the NSP2 CHF correlation in VIPRE-01, within its range of applicability in Table 7-2, along with its associated correlation limit of 1.17, for the NuScale Design Certification Application (DCA) and safety analysis of the NuScale Power Module (NPM) with NuFuel-HTP2™ fuel. This correlation conforms to acceptance criteria given by the NuScale Design-Specific Review Standard (DSRS), and the requirements of 10 CFR 50, Appendix A, General Design Criterion (GDC) 10.

This topical report presents the NSP2 critical heat flux (CHF) correlation developed by NuScale to assess CHF performance for normal operation and anticipated operational occurrences (AOOs) in the NPM with NuFuel-HTP2™ fuel. Described in this report are the tests, test facilities, statistical methods, correlation development process, and resultant NSP2 CHF correlation.

The NPM will use the NuFuel-HTP2™ fuel assembly design for the DCA. This fuel assembly is a half-height, standard 17x17 design that includes AREVA's HMP™ and HTP™ spacer grids. The NSP2 CHF correlation developed within this report is used with this fuel design.

The CHF tests for NuScale were performed at Stern Laboratories, Inc. in Ontario, Canada and at AREVA's Karlstein, Germany thermal-hydraulic (KATHY) test facility to obtain steady-state CHF data used in the derivation and validation of the NSP2 CHF correlation. The Stern tests were performed on a preliminary prototypical bundle geometrically comparable to the NuFuel-HTP2™ design, but with {{ }}[2(a),(c)]. The Stern preliminary prototypical bundle tests provide data over wide parameter ranges, which encompass the NPM operating parameter values that are analyzed with the VIPRE-01 code, to develop a base CHF correlation. A set of existing CHF data for an HMP™ spacer grid (KATHY K8500 HMP™), which is utilized in the NuFuel-HTP2™ design, is used to develop an "NSPX factor" that conservatively predicts the NuFuel-HTP2™ CHF performance. The NSP2 CHF correlation combines the base CHF correlation and this NSPX factor. The CHF tests of the reference NuFuel-HTP2™ design were conducted by AREVA at the KATHY test facility (KATHY NuFuel-HTP2™) to provide data to validate the NSP2 CHF correlation for the NPM application. Overall, data were obtained from {{ }}[2(a),(c)] separate CHF tests including {{ }}[2(a),(c)] along with both unit and guide tube layouts. A total of {{ }}[2(a),(c)] data points are used to develop the CHF correlation form, coefficients and NSPX factor while {{ }}[2(a),(c)] data points are used to validate the CHF correlation for NuFuel-HTP2™ fuel.

The figure of merit for preventing the occurrence of CHF in the NPM is critical heat flux ratio (CHFR), rather than departure from nucleate boiling ratio that is traditionally used for pressurized water reactor (PWR) applications. The CHFR is used for consistency in modeling the range of NuScale specific phenomena, and is defined as the ratio of CHF to local heat flux. The NSP2 CHF correlation that has been developed is an empirical based correlation that takes into account fuel geometry and local fluid conditions, properties and heat flux. It includes a non-uniform flux factor (FNU) that accommodates variability in axial power profiles in the NPM. The NSP2 CHF correlation conservatively predicts {{ }}[2(a),(c)]. Therefore, the NSP2 CHF correlation conservatively predicts CHF for the NuFuel-HTP2™ application in the NPM, when used in conjunction with the applicable statistically derived correlation limit. Application of a CHFR limit determined with the NSP2 CHF correlation, ensures with a 95 percent probability at the 95 percent confidence level (95/95 level), that the hot fuel rod in the core does not experience CHF during normal operation or AOOs in conformance with the acceptance criteria given by the NuScale DSRS, Section 4.4 (Reference 8.1.3). The application of this CHF correlation to safety analysis, including development of safety analysis design limits, application of uncertainties or fuel failure methods, is outside of the scope of this report.

The NSP2 CHF correlation will be used in safety analysis evaluations of the NPM using the NuFuel-HTP2™ fuel design with local conditions calculated by the VIPRE-01 subchannel thermal-hydraulic code. Qualification of VIPRE-01 for use in NPM calculations is addressed in the NuScale Subchannel Analysis Methodology topical report (Reference 8.2.3).

1.0 Introduction

1.1 Purpose

This report presents the NSP2 critical heat flux (CHF) correlation that has been developed by NuScale to assess CHF performance for normal operation and anticipated operational occurrences (AOOs) in the NuScale Power Module (NPM) with NuFuel-HTP2™ fuel. This report describes the tests, test facilities, statistical methods, and CHF correlation development process. NuScale requests NRC approval of the NSP2 CHF correlation in VIPRE-01, within its range of applicability in Table 4-5, along with its associated correlation limit of 1.17, for the NuScale DCA and safety analysis of the NPM with NuFuel-HTP2™ fuel.

1.2 Scope

This report presents descriptions of the NuScale CHF testing, and the development and validation of the NSP2 CHF correlation. The overall process flow is illustrated in Figure 1-1. The facilities and test descriptions are provided in Section 3.1 along with methods for obtaining data. The development of the base CHF correlation and NSPX factor that make up the NSP2 CHF correlation are presented in Section 4.0 and 5.0, respectively. Development of a {{ }}$^{2(a),(c)}$ is discussed in Section 4.3. Validation of the NSP2 CHF correlation with NuFuel-HTP2™ design specific CHF test data is presented in Section 6.0.

The application of this CHF correlation to safety analysis, including the development of safety analysis design limits, application of uncertainties or fuel failure survey methods, is outside of the scope of this report.

The CHF correlation is based upon {{ }}$^{2(a),(c)}$ Qualification of VIPRE-01 for use in NPM calculations is outside of the scope of this report and is addressed in the NuScale Subchannel Analysis Methodology Topical Report (Reference 8.2.3). The two-phase and heat transfer correlations used for deriving local conditions (refer to Section 3.3.1) in this report are consistent with those in Reference 8.2.3. Use of the CHF correlation developed in this report requires consistency with the VIPRE-01 two-phase and heat transfer correlations in Section 3.3.1 of this report and Reference 8.2.3.

{{

}}2(a),(c)

Figure 1-1. CHF correlation development flow chart

NuScale Nonproprietary

1.3 Abbreviations

Table 1-1. Abbreviations

Term	Definition
AOO	anticipated operational occurrence
BOHL	beginning of heated length
BWR	boiling water reactor
CHF	critical heat flux
CHFR	critical heat flux ratio
DAS	data acquisition system
DCA	Design Certification Application
DSRS	Design Specific Review Standard
EOHL	end of heated length
FNU	non-uniform flux factor
GDC	General Design Criterion
M/P	measured-to-predicted ratio
NRC	U.S. Nuclear Regulatory Commission
NPM	NuScale Power Module
P/M	predicted-to-measured ratio
PWR	pressurized water reactor
RTD	resistance temperature detectors

Table 1-2. Definitions

Term	Definition
95/95 Level	95% probability at the 95% confidence level
Bartlett Test	The *Bartlett test* is used for testing the homoscedasticity of several populations.
C1	CHF unit test with {{ }}$^{2(a),(c)}$ conducted at Stern Laboratories for preliminary prototypical bundle design
{{ }}$^{2(a),(c)}$	{{ }}$^{2(a),(c)}$
{{ }}$^{2(a),(c)}$	{{ }}$^{2(a),(c)}$
D'Agostino (*D'*) Test	The *D'Agostino test*, or *D'* test, tests whether the distribution from which a sample is taken is a normal distribution (Reference 8.2.1, Section 11.10). This test may be used for sample sizes of 50 or more.
Guide Tube Test	Test section where the four central subchannels are surrounded by 3 heated rods and 1 guide tube while the remaining subchannels are surrounded by 4 heated rods except the wall subchannels
K8500	CHF **[** **]** conducted by AREVA

NuScale Nonproprietary

Term	Definition
K9000	CHF {{ }}2(a),(c) conducted by AREVA
K9100	CHF {{ }}2(a),(c) conducted by AREVA
K9200	CHF {{ }}2(a),(c) conducted by AREVA
K9300	CHF {{ }}2(a),(c) conducted by AREVA
KATHY	Areva's Karlstein thermal-hydraulic test facility
Kruskal-Wallis Test	The *Kruskal-Wallis test* is a non-parametric method for testing whether two or more independent samples of equal or different sizes originate from the same distribution. This test has an underlying assumption of equal variances.
Level of Significance	Level of significance is the acceptable level of risk of rejecting the null hypothesis when the null hypothesis is actually correct
Median Test	The *Median test* is a non-parametric method for testing whether two or more independent samples of equal or different sizes originate from the same distribution. This test has no assumption of equal variances.
Null Hypothesis	The null hypothesis is a statement describing a populations parameters that can be tested
NuScale Power Module	The NPM is a self-contained nuclear steam supply system composed of a reactor core, a pressurizer, and two steam generators integrated within the reactor pressure vessel and housed in a compact steel containment vessel.
Parametric and Non-parametric	A distribution (Reference 8.2.1, Section 25.2) is considered parametric if the form of the distribution is known (e.g. belongs to a normal distribution or another with known parameters). If the form of the distribution is not known, and the central limit theorem is not applicable, then the distribution is considered non-parametric.
Population	A population (Reference 8.2.1, Section 1.6) is a collection of measurements made on items defined by some characteristic of the items. At least a single observation (e.g. pressure, mass flux, CHF) is associated with each item (or statistic).
Shapiro-Wilks (*W*) Test	The *Shapiro Wilk test*, or *W-test*, tests whether the distribution from which a sample is taken is a normal distribution (Reference 8.2.1, Section 11.9). This test may be used for sample sizes below 50.
Tolerance Limits	Statistical tolerance limits have the property that a specified percentage of the population is expected to fall within them (Reference 8.2.1, Section 9.12) with a specified confidence.
U1	CHF unit test with {{ }}2(a),(c) conducted at Stern Laboratories for preliminary prototypical bundle design
U2	CHF guide tube test with {{ }}2(a),(c) conducted at Stern Laboratories for preliminary prototypical bundle design
Unit Test	Test section where all of the subchannels are surrounded by four heated rods except the wall subchannels

NuScale Nonproprietary

2.0 Background

In a pressurized water reactor (PWR), the majority of heat generated in the fuel pellets is conducted through the fuel rod materials to be removed by convective heat transfer to the water coolant. Reactors are designed to operate at a point where this heat transfer to the coolant occurs in either sub-cooled or nucleate boiling conditions, both of which provide efficient means of heat transfer. The condition of the coolant adjacent to the cladding surface may transition to a condition where a continuous vapor layer separates the fuel rod surfaces from the coolant in off-nominal conditions, such as AOOs and postulated accidents. Under these conditions, heat transfer to the coolant is degraded due to the decreased heat transfer coefficient. The rod surface heat flux corresponding to the point of transition to boiling crisis is referred to as the CHF. The reduction in heat transfer to the coolant at these conditions results in an increase in fuel rod temperatures that could challenge fuel rod cladding integrity. A design specific CHF correlation is developed for use in safety analyses of the NPM to assure that this will not occur.

The NPM is a self-contained nuclear steam supply system composed of an integral reactor core, two helical-coil steam generators and pressurizer within the reactor pressure vessel and housed in a compact steel containment. It is designed to operate under natural circulation to provide primary coolant flow, which eliminates the need for reactor coolant pumps. This reactor design results in significantly lower core coolant flow rates than conventional PWR designs, and also operates at a lower system pressure than conventional PWR designs. The NPM relies on the NuFuel-HTP2™ fuel design, which uses AREVA's HTP™ and HMP™ spacer grid technology. Development of a fuel assembly design specific CHF correlation is required to characterize these design and operating conditions and to provide a correlation for analyzing the thermal performance of the NPM.

A CHF correlation is dependent on the fuel assembly design: fuel and guide tube diameters, rod pitch, spacer grid design, spacer grid pitch, etc. It is also dependent on its application: pressures, mass fluxes, inlet subcooling, etc. The CHF is typically predicted with a correlation based on empirical data from design-specific CHF testing that addresses these dependencies. Such testing generally models the fuel designs in full axial scale with a scaled radial lattice (i.e. 5x5 in testing rather than 15x15 or 17x17 in production). The CHF testing is conducted over a wide range of operating conditions, generally encompassing the ranges experienced during normal reactor operation and AOOs.

Initial CHF testing for the NPM at Stern Laboratories was performed on a preliminary prototypical design that was geometrically similar to the NuFuel-HTP2™ design, but was equipped with {{ }}[2(a),(c)]. These tests were performed at fluid conditions appropriate for the NPM and were used to develop the base CHF correlation. The "NSPX factor" is developed using {{ }}[2(a),(c)] for the NPM, in order to apply this base correlation to the NuFuel-HTP2™ design while {{ }}[2(a),(c)]. The base correlation combined

with the NSPX factor forms the basis of the NSP2 CHF correlation. Adequacy of the NSP2 CHF correlation is assessed with NuFuel-HTP2™ design specific CHF test data from AREVA's KATHY test facility.

2.1 Regulatory Requirements

Failure of nuclear fuel rods must be precluded in accordance with 10 CFR 50, Appendix A, GDC 10 (Reference 8.1.1).

Specified acceptable fuel design limits based on CHF conditions are established to prevent degradation of heat transfer from the fuel rod surface, which could cause an increase in temperatures that may ultimately lead to the failure of the fuel rod cladding. As discussed above, the NPM design is required to assure that these limits are not exceeded during normal operation or AOOs.

The NuScale Design Specific Review Standard (DSRS) (Reference 8.1.3), Section 4.4, provides specific criteria necessary to meet the requirements of GDC 10. For CHF correlations, there should be a 95-percent probability at the 95-percent confidence level (95/95 level) that the hot rod in the core does not experience a boiling crisis during normal operation or AOOs.

2.2 NuScale Power Module Fuel Assembly Design

The NPM utilizes the NuFuel-HTP2™ fuel assembly, illustrated in Figure 2-1, which uses AREVA's HMP™ and HTP™ spacer grids. The spacer grids, illustrated in Figure 2-2 and Figure 2-3, are located axially at locations indicated in Table 2-1. Principle fuel assembly parameters are tabulated in Table 2-1.

Table 2-1. NuFuel-HTP2™ fuel assembly parameters

Parameter	Value
Fuel assembly layout	17 x 17
Fuel rod outer diameter	0.374 in.
Fuel rod pitch	0.496 in.
Guide tube outer diameter	0.482 in.
Number of fuel rods per bundle	264
Number of guide tubes per bundle	24
Number of instrument tubes per bundle	1
Length of total active fuel stack	78.74 in.
Grid spacer height	1.750 in.
Axial spacing from bottom of heated length to centerline of grid spacer	{{ }}2(a),(c),ECI {{ }}2(a),(c),ECI {{ }}2(a),(c),ECI {{ }}2(a),(c),ECI {{ }}2(a),(c),ECI

[1] Note that {{ }}2(a),(c)

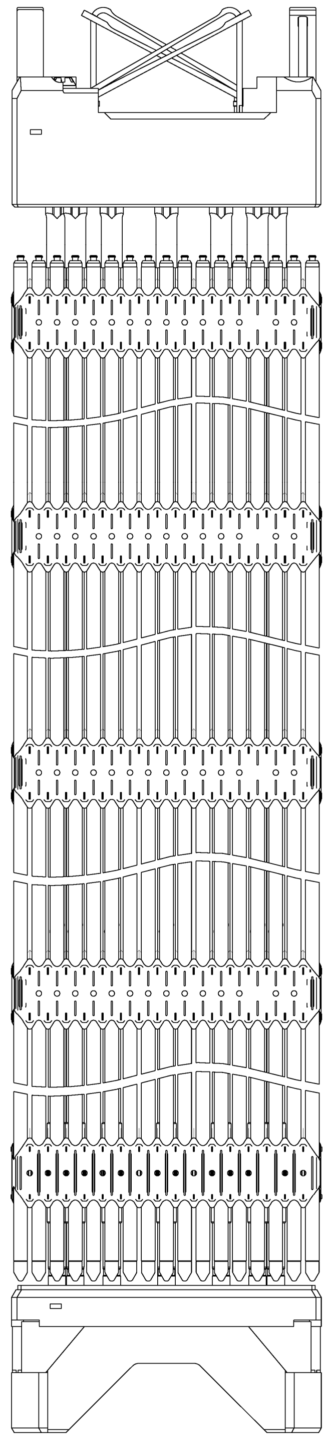

Figure 2-1. NuFuel-HTP2™ fuel assembly

NuScale Nonproprietary

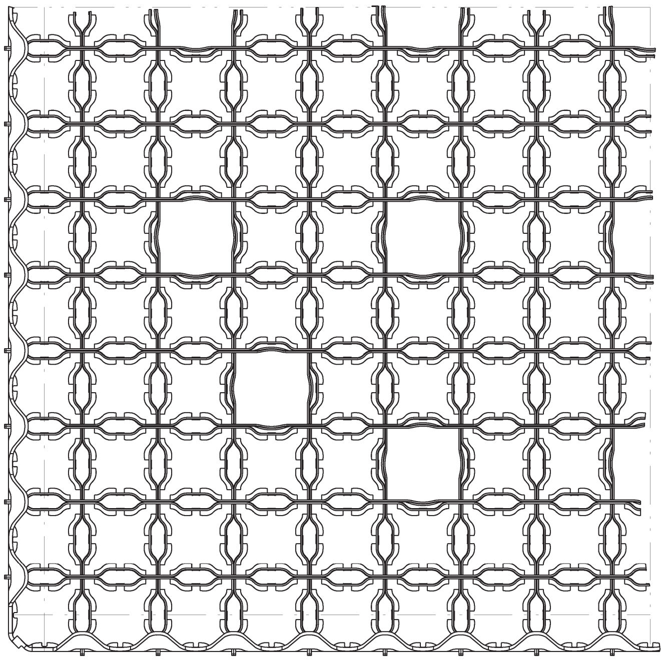

Figure 2-2. HMP™ spacer grid ($^1/_4$ of grid shown)

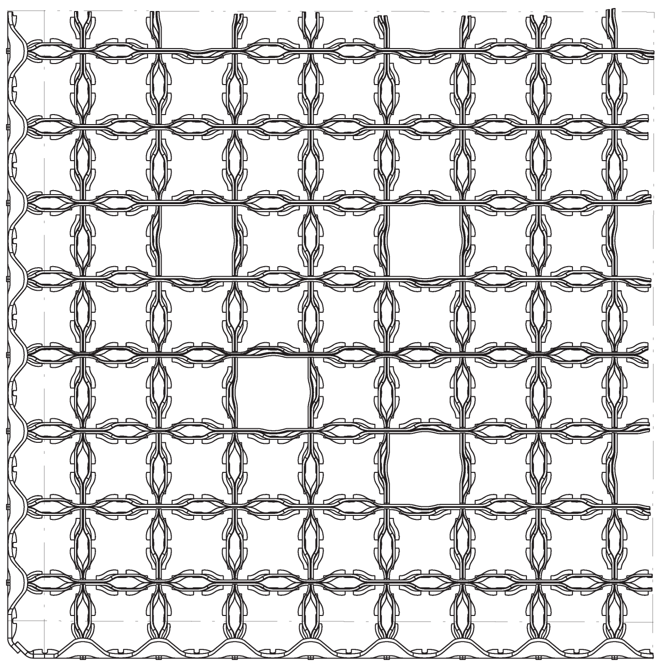

Figure 2-3. HTP™ spacer grid ($^1/_4$ of grid shown)

3.0 Analysis and Experimentation

3.1 Data Sources

3.1.1 Stern Laboratories

The CHF testing was performed on a preliminary prototypical design for NuScale by Stern Laboratories in Ontario, Canada between September 2012 and March 2013. Three tests, referenced as U1, U2 and C1, were performed. The U1 test is a unit test with {{ }}$^{2(a),(c)}$. The U2 test is a guide tube test with {{ }}$^{2(a),(c)}$. The C1 test is a unit test with {{ }}$^{2(a),(c)}$. These tests are discussed in the NuScale Critical Heat Flux Test Program Technical Report (Reference 8.2.2). The following sections describe the test section, the test loop and the instrumentation utilized in the test campaign. The test matrix corresponding to the tests performed at Stern Laboratories for the test campaign is tabulated in Table 3-1.

Table 3-1. Stern preliminary prototypical test matrix

{{

}}$^{2(a),(c),ECI}$

{{

}}2(a),(c),ECI

3.1.1.1 Stern Preliminary Prototypic Test Section

The test section, illustrated schematically in Figure 3-1, consists of pressure housing, flow channel of square cross section, the fuel simulation, and instrumentation. The fuel simulation is a 5x5 array of electrically heated rods with parameters described in Table 3-2. The pressure housing is designed for {{ }}2(a),(c). The pressure housing is {{ }}2(a),(c) long and has re-entrant geometries at the inlet and outlet of the test section to provide calming regions to minimize potential flow maldistribution. The simulated fuel rods are fastened in a manner that allows for thermal expansion. The flow channel design allows for thermal expansion and reduces mixing of the main flow stream with the water in the annulus formed between the flow channel and the pressure housing.

The fuel simulation utilizes twenty-five fuel simulators (or twenty-four plus a central unheated tube in guide tube tests) assembled into a 5x5 square array with rods positioned using spacer grids. The spacer grids, illustrated in Figure 3-2 and Figure 3-3, are located axially at locations indicated in Table 3-2. The axial positioning of the grid spacers, illustrated in Figure 3-1, indicates that the distance between grid spacers varies between {{ }}2(a),(c),ECI The indirectly heated fuel simulators in the U1 and U2 test series have a {{ }}2(a),(c), ECI while those in the C1

test series have a {{ }}2(a),(c), ECI. The {{ }}2(a),(c), ECI:

{{

Eq. 3-1

}}2(a),(c)

where,

{{ }}2(a),(c)

{{ }}2(a),(c)

{{ }}2(a),(c)

$z =$ axial location relative to the beginning of the heated length, in.

{{ }}2(a),(c)

The radial peaking distribution for the U1, C1 and U2 tests are illustrated in Figure 3-4 and Figure 3-5.

Table 3-2. Stern Laboratories test section physical parameters

Parameter	U1	U2	C1
Flow channel width		{{ }}2(a),(c),ECI	
Fuel simulator diameter		{{ }}2(a),(c),ECI	
{{ }}2(a),(c),ECI	-	{{ . }}2(a),(c),ECI	-
Grid heater rod pitch		{{ }}2(a),(c),ECI	
Heated length		{{ }}2(a),(c),ECI	
Axial power distribution	{{ }}2(a),(c),ECI	{{ }}2(a),(c),ECI	{{ }}2(a),(c),ECI
Grid spacer height		{{ }}2(a),(c)	
{{ }}2(a),(c)[2]		Grid #1: {{ }}2(a),(c) Grid #2: {{ }}2(a),(c) Grid #3: {{ }}2(a),(c) Grid #4: {{ }}2(a),(c) Grid #5: {{ }}2(a),(c)	
{{ }}2(a),(c)		{{ }}2(a),(c) {{ }}2(a),(c) {{ }}2(a),(c) {{ }}2(a),(c) {{ }}2(a),(c)	

Note: {{ }}2(a),(c).

[2] Note that {{ }}2(a),(c)

{{

}}2(a),(c), ECI

Figure 3-1. Stern Laboratories test section axial schematic

{{

}}2(a),(c),ECI

Figure 3-2. Stern Laboratories U1 and C1 grid spacer

{{

}}2(a),(c), ECI

Figure 3-3. Stern Laboratories U2 grid spacer

{{

}}2(a),(c), ECI

Figure 3-4. Stern Laboratories U1 and C1 test radial schematic

{{

}}2(a),(c), ECI

Figure 3-5. Stern Laboratories U2 test radial schematic

3.1.1.2 Stern Laboratories Test Loop

The Stern Laboratories test facility is used for collecting thermal-hydraulic test data for pressurized water and boiling water reactors. The test loop schematic is illustrated in Figure 3-6.

The Stern Laboratories loop design pressure and temperature are {{ }}$^{2(a),(c)}$, respectively. Loop coolant circulation flow is provided by a high head, high capacity pump with flow adjusted by control valves at the inlet to the test section. The pressure is maintained at the test section outlet (downstream end of heated length) using a pressurizer.

The Stern Laboratories test loop's electric power supply has a maximum power of approximately {{ }}$^{2(a),(c)}$. Three of the {{ }}$^{2(a),(c)}$ power supplies can be used in reversed polarity to minimize the magnetic forces due to electric current. The power supplies are low ripple, twelve pulse design and employ current feedback for stable control.

{{

}}2(a),(c)

Note: Figure provided for illustration purposes only. Illegible text is not pertinent.

Figure 3-6. Stern Laboratories PWR test loop schematic

3.1.1.3 Stern Laboratories Instrumentation and Data Acquisition System

The test section and loop are instrumented to measure power, flow rates, absolute pressures, differential pressures, and coolant and fuel simulator temperatures during testing. Pressure transmitters are used to measure absolute and differential pressures. Pressure taps are installed {{ }}[2(a),(c)]. Resistance temperature detectors (RTDs) are used to measure {{ }}[2(a),(c)] of the test section. Thermal wells are installed into the piping for the RTDs to measure the coolant temperature. The flow rate is measured using {{ }}[2(a),(c)]. The flow, pressure, differential pressure and temperature measurement devices used during the experiments were in current calibration.

The fuel simulators are instrumented with {{ }}[2(a),(c)]. The axial locations of the {{ }}[2(a),(c)] are illustrated in Figure 3-1. The {{ }}[2(a),(c)] for each test series are illustrated in Figure 3-7 and Figure 3-8.

{{ }}[2(a),(c)] during the thermal mixing tests. The identification and location of the {{ }}[2(a),(c)] for each test series are illustrated in Figure 3-9 and Figure 3-10.

Current and voltage transducers are used to measure the amperage and voltage {{ }}[2(a),(c)]. These measurements are used to calculate the actual fuel simulator power and peaking factors.

The laboratory data acquisition system (DAS) is used to scan the instruments and convert the signals to engineering units and perform various calculations. A list of the DAS measurements and calculations and their associated uncertainties are tabulated in Table 3-3. The instrument signals are scanned continuously at the rate of 10 Hz per channel and selected channels are displayed on video monitors. For steady-state tests, signals are recorded for a period of 30 seconds and the averages are calculated in engineering units. For critical power tests, when the operator initiates a data recording event, a 20 second pre-event data buffer and a 20 second post-event data recording are stored. If the power control program initiates a power step down due to a {{ }}[2(a),(c)] the data are automatically stored by the DAS in the same manner as the critical power data recording.

The data acquisition program continuously scans the {{ }}2(a),(c) and utilizes various software algorithms and graphical techniques to ensure that the first occurrence of CHF is detected.

A calculated {{ }}2(a),(c) is used for predicting the occurrence of CHF. Routinely during testing, a user-initiated software procedure (normalization) estimates {{ }}2(a),(c). Using the {{ }}2(a),(c) ensured a discernible and consistent CHF criterion was applied. Following the normalization procedure described above just prior to CHF, the {{ }}2(a),(c) throughout a given axial plane of the fuel simulation were all within {{ }}2(a),(c) of each other. At the onset of CHF, when the heat transfer coefficient intermittently begins to deteriorate, small perturbations {{ }}2(a),(c) are observed. As the power is increased {{ }}2(a),(c) as the mechanism of heat transfer approaches film boiling. The CHF criterion is met when any of the {{ }}2(a),(c), which experience has shown to be sufficient to differentiate from noise and still below the boiling crisis when rapid excursions occur.

Heat balance tests were performed to check the consistency of the primary measurements and assure that the test equipment was operating within the expected parameters. The heat balance is expressed in terms of heat loss and was typically less than {{ }}2(a),(c). Therefore, for development of the base CHF correlation these heat losses are ignored.

Table 3-3. Stern Laboratories DAS variables and uncertainties

Measurement / Calculation	Units	Method	Uncertainty
Test section inlet temperature	°C	{{ }}2(a),(c)	{{ }}2(a),(c)
Test section outlet pressure	kPa	{{ }}2(a),(c)	{{ }}2(a),(c)
Test section mass flux	kg/s-m^2	{{ }}2(a),(c)	{{ }}2(a),(c)
Total measured power	kW	{{ }}2(a),(c)	{{ }}2(a),(c)

{{

}}2(a),(c),ECI

Figure 3-7. Stern preliminary prototypic U1 and U2 test sections thermocouple layout

{{

}}2(a),(c),ECI

Figure 3-8. Stern preliminary prototypic C1 test section thermocouple layout

NuScale Nonproprietary

{{

}}2(a),(c),ECI

Figure 3-9. Stern preliminary prototypic U1 and C1 thermal mixing thermocouples

{{

}}2(a),(c),ECI

Figure 3-10. Stern preliminary prototypic U2 thermal mixing thermocouples

NuScale Nonproprietary

3.1.2 AREVA

AREVA provided NuScale with CHF data from testing at the KATHY test facility in Karlstein, Germany. Data was provided for the HMP™ spacer grid design from the KATHY K8500 test **[ ]** conducted in December of 2014. The test assembly has similar geometry to that of the NuFuel-HTP2™ fuel design {{ }}$^{2(a),(c),ECI}$ and thermal-hydraulic conditions that fall within the range of pressure and mass flux tested for the Stern preliminary prototypical bundle. The KATHY K8500 HMP™ test provides representative data to assess the base CHF correlation for the NuFuel-HTP2™ fuel design and develop the NSPX factor (refer to Section 5.2). While the KATHY K8500 HMP™ test data are based on HMP™ spacer grids and the NuFuel-HTP2™ design relies on both HMP™ and HTP™ spacer grids, the data are considered applicable because {{ }}$^{2(a),(c)}$.

Testing of the reference NuFuel-HTP2™ fuel design was performed by AREVA at the KATHY test facility between March and July of 2016. Four tests, referenced as K9000, K9100, K9200, and K9300, were performed during this campaign.

- K9000 is a {{ }}$^{2(a),(c)}$
- K9100 is a {{ }}$^{2(a),(c)}$
- K9200 is a {{ }}$^{2(a),(c)}$
- K9300 is a {{ }}$^{2(a),(c)}$

The test matrix performed for the KATHY NuFuel-HTP2™ tests is tabulated in Table 3-4. Unlike testing for the Stern preliminary prototypical design, data (refer to Table 3-1) were not taken at every statepoint in the test matrix for each of the tests. Instead, data points were spread out among the four tests. In the end each statepoint is covered by at least one test. The test matrix is designed so that there is overlap between {{ }}$^{2(a),(c)}$. There is also overlap between guide tube and unit tests.

Table 3-4. Test matrix for KATHY NuFuel-HTP2™ testing

{{

}}2(a),(b),(c)

3.1.2.1 KATHY K8500 HMP™ Test Section

The KATHY K8500 HMP™ test section is comprised of twenty-five fuel simulators assembled into a 5x5 square array with HMP™ spacer grids. The spacer grids are located axially at locations indicated in Table 3-5. **[**

]. The number and locations of the spacer grids are tabulated in Table 3-5 and illustrated in Figure 3-11. The fuel simulators in the KATHY K8500 HMP™ test have a **[** **]**ECI. The radial power distribution is illustrated in Figure 3-11. The number and location of the **[** **]** are also tabulated in Table 3-5 and illustrated in Figure 3-11.

Table 3-5. KATHY K8500 HMP™ test section physical parameters

Parameter	Value
Flow channel width	**[ ]**ECI
Fuel simulator diameter	**[ ]**ECI
Grid heater rod pitch	**[ ]**ECI
Heated length	**[ ]**ECI
Axial power distribution	**[ ]**ECI
Grid spacer height	**[ ]**ECI
Axial spacing from BOHL to bottom of HMP™ spacer grid[3]	Grid #1: **[ ]** Grid #2: **[ ]** Grid #3: **[ ]** Grid #4: **[ ]** Grid #5: **[ ]**
Axial spacing from BOHL to bottom of support grid	Grid #1: **[ ]** Grid #2: **[ ]** Grid #3: **[ ]** Grid #4: **[ ]**
[ ]ECI	**[ ]** **[ ]** **[ ]** **[ ]** **[ ]** **[ ]** **[ ]**

[3] Only spacer grids {{ }}2(a),(c) are modeled in VIPRE-01

[

]EC1

Figure 3-11. KATHY K8500 HMP™ test section schematic

3.1.2.2 KATHY NuFuel-HTP2™ K9000 Test Section

The K9000 test section represents the NuFuel-HTP2™ fuel design and is comprised of twenty-four fuel simulators and a central guide tube assembled into a 5x5 square array with HMP™ and HTP™ spacer grids. The spacer grids are located axially at locations indicated in Table 3-6. {{ }}$^{2(a),(c)}$. The number and locations of the spacer grids are tabulated in Table 3-6 and illustrated in Figure 3-12. The fuel simulators in the K9000 test have a {{ }}$^{2(a),(c),ECI}$. The radial power distribution is illustrated in Figure 3-12. The number and location of the {{ }}$^{2(a),(c)}$ are also tabulated in Table 3-6 and illustrated in Figure 3-12.

Table 3-6. KATHY NuFuel-HTP2™ K9000 test section physical parameters

Parameter	Value
Flow channel width	{{ }}$^{2(a),(c),ECI}$
Fuel simulator diameter	{{ }}$^{2(a),(c),ECI}$
{{ }}$^{2(a),(c),ECI}$	{{ }}$^{2(a),(c),ECI}$
Grid heater rod pitch	{{ }}$^{2(a),(c),ECI}$
Heated length	{{ }}$^{2(a),(c),ECI}$
Axial power distribution	{{ }}$^{2(a),(c),ECI}$
HTP™ spacer grid height	{{ }}$^{2(a),(c),ECI}$
HMP™ spacer grid height	{{ }}$^{2(a),(c),ECI}$
{{ }}$^{2(a),(c),ECI}$	{{ }}$^{2(a),(c),ECI}$
Axial spacing from BOHL to bottom of HTP™ grid spacer[4]	Grid #1: {{ }}$^{2(a),(c)}$ Grid #2: {{ }}$^{2(a),(c)}$ Grid #3: {{ }}$^{2(a),(c)}$
Axial spacing from BOHL to bottom of support grid	Grid #1: {{ }}$^{2(a),(c)}$ Grid #2: {{ }}$^{2(a),(c)}$ Grid #3: {{ }}$^{2(a),(c)}$ Grid #4: {{ }}$^{2(a),(c)}$
{{ }}$^{2(a),(c),ECI}$	{{ }}$^{2(a),(c)}$ {{ }}$^{2(a),(c)}$ {{ }}$^{2(a),(c)}$ {{ }}$^{2(a),(c)}$

[4] Only spacer grids {{ }}$^{2(a),(c)}$ are modeled in VIPRE-01

{{

}}2(a),(c),ECI

Figure 3-12. KATHY NuFuel-HTP2™ K9000 test section schematic

3.1.2.3 KATHY NuFuel-HTP2™ K9100 Test Section

The K9100 test section represents the NuFuel-HTP2™ fuel design and is comprised of twenty-five fuel simulators assembled into a 5x5 square array with HMP™ and HTP™ spacer grids. The spacer grids are located axially at locations indicated in Table 3-7. As with other KATHY tests, {{ }}$^{2(a),(c)}$. The number and locations of the spacer grids are tabulated in Table 3-7 and illustrated in Figure 3-13. The fuel simulators in the K9100 test have a {{ }}$^{2(a),(c),ECI}$. The radial power distribution is illustrated in Figure 3-13. The number and location of the {{ }}$^{2(a),(c)}$ are also tabulated in Table 3-7 and illustrated in Figure 3-13.

Table 3-7. KATHY NuFuel-HTP2™ K9100 test section physical parameters

Parameter	Nominal Value
Flow channel width	{{ }}$^{2(a),(c),ECI}$
Fuel simulator diameter	{{ }}$^{2(a),(c),ECI}$
{{ }}$^{2(a),(c),ECI}$	{{ }}$^{2(a),(c),ECI}$
Grid heater rod pitch	{{ }}$^{2(a),(c),ECI}$
Heated length	{{ }}$^{2(a),(c),ECI}$
Axial power distribution	{{ }}$^{2(a),(c),ECI}$
HTP™ spacer grid height	{{ }}$^{2(a),(c),ECI}$
HMP™ spacer grid height	{{ }}$^{2(a),(c),ECI}$
{{ }}$^{2(a),(c),ECI}$	{{ }}$^{2(a),(c),ECI}$
Axial spacing from BOHL to bottom of HTP™ grid spacer[5]	Grid #1: {{ }}$^{2(a),(c)}$ Grid #2: {{ }}$^{2(a),(c)}$ Grid #3: {{ }}$^{2(a),(c)}$
Axial spacing from BOHL to bottom of support grid	Grid #1: {{ }}$^{2(a),(c)}$ Grid #2: {{ }}$^{2(a),(c)}$ Grid #3: {{ }}$^{2(a),(c)}$ Grid #4: {{ }}$^{2(a),(c)}$
{{ }}$^{2(a),(c),ECI}$	{{ }}$^{2(a),(c)}$ {{ }}$^{2(a),(c)}$ {{ }}$^{2(a),(c)}$ {{ }}$^{2(a),(c)}$

[5] Only spacer grids {{ }}$^{2(a),(c)}$ are modeled in VIPRE-01

{{

}}2(a),(c),ECI

Figure 3-13. KATHY NuFuel-HTP2™ K9100 test section schematic

3.1.2.4 KATHY NuFuel-HTP2™ K9200 Test Section

The K9200 test section represents the NuFuel-HTP2™ fuel design and is comprised of twenty-four fuel simulators and a central guide tube assembled into a 5x5 square array with HMP™ and HTP™ spacer grids. The spacer grids are located axially at locations indicated in Table 3-8. As with other KATHY tests, {{

}}$^{2(a),(c)}$. The number and locations of the spacer grids are tabulated in Table 3-8 and illustrated in Figure 3-14. The fuel simulators in the K9200 test have a {{ }}$^{2(a),(c),ECI}$, which is described in Table 3-9. The radial power distribution is illustrated in Figure 3-14. The number and location of the {{ }}$^{2(a),(c)}$ are also tabulated in Table 3-8 and illustrated in Figure 3-14.

Table 3-8. KATHY NuFuel-HTP2™ K9200 test section physical parameters

Parameter	Value
Flow channel width	{{ }}$^{2(a),(c),ECI}$
Fuel simulator diameter	{{ }}$^{2(a),(c),ECI}$
{{ }}$^{2(a),(c),ECI}$	{{ }}$^{2(a),(c),ECI}$
Grid heater rod pitch	{{ }}$^{2(a),(c),ECI}$
Heated length	{{ }}$^{2(a),(c),ECI}$
Axial power distribution	{{ }}$^{2(a),(c),ECI}$
HTP™ spacer grid height	{{ }}$^{2(a),(c),ECI}$
HMP™ spacer grid height	{{ }}$^{2(a),(c),ECI}$
{{ }}$^{2(a),(c),ECI}$	{{ }}$^{2(a),(c),ECI}$
Axial spacing from BOHL to bottom of HTP™ grid spacer[6]	Grid #1: {{ }}$^{2(a),(c)}$ Grid #2: {{ }}$^{2(a),(c)}$ Grid #3: {{ }}$^{2(a),(c)}$ Grid #4: {{ }}$^{2(a),(c)}$
Axial spacing from BOHL to bottom of support grid	Grid #1: {{ }}$^{2(a),(c)}$ Grid #2: {{ }}$^{2(a),(c)}$ Grid #3: {{ }}$^{2(a),(c)}$ Grid #4: {{ }}$^{2(a),(c)}$
{{ }}$^{2(a),(c),ECI}$	{{ }}$^{2(a),(c)}$ {{ }}$^{2(a),(c)}$ {{ }}$^{2(a),(c)}$ {{ }}$^{2(a),(c)}$ {{ }}$^{2(a),(c)}$ {{ }}$^{2(a),(c)}$

[6] Only spacer grids {{ }}$^{2(a),(c)}$ are modeled in VIPRE-01

Table 3-9. KATHY NuFuel-HTP2™ K9200 axial power profile

{{

}}2(a),(c),ECI

{{

}}2(a),(c),ECI

Figure 3-14. KATHY NuFuel-HTP2™ K9200 test section schematic

3.1.2.5 KATHY NuFuel-HTP2™ K9300 Test Section

The K9300 test section represents the NuFuel-HTP2™ fuel design and is comprised of twenty-five fuel simulators assembled into a 5x5 square array with HMP™ and HTP™ spacer grids. The spacer grids are located axially at locations indicated in Table 3-10. As with other KATHY tests, {{ }}[2(a),(c)]. The number and locations of the spacer grids are tabulated in Table 3-10 and illustrated in Figure 3-15. The fuel simulators in the K9300 test have a {{ }}[2(a),(c),ECI], which is described in Table 3-9. The radial power distribution is illustrated in Figure 3-15. The number and location of the {{ }}[2(a),(c)] are also tabulated in Table 3-10 and illustrated in Figure 3-15.

Table 3-10. KATHY NuFuel-HTP2™ K9300 test section physical parameters

Parameter	Value
Flow channel width	{{ }}2(a),(c),ECI
Fuel simulator diameter	{{ }}2(a),(c),ECI
Grid heater rod pitch	{{ }}2(a),(c),ECI
Heated length	{{ }}2(a),(c),ECI
Axial power distribution	{{ }}2(a),(c),ECI
HTP™ spacer grid height	{{ }}2(a),(c),ECI
HMP™ spacer grid height	{{ }}2(a),(c),ECI
{{ }}2(a),(c),ECI	{{ }}2(a),(c),ECI
Axial spacing from BOHL to bottom of HTP™ grid spacer[7]	Grid #1: {{ }}2(a),(c) Grid #2: {{ }}2(a),(c) Grid #3: {{ }}2(a),(c) Grid #4: {{ }}2(a),(c)
Axial spacing from BOHL to bottom of support grid	Grid #1: {{ }}2(a),(c) Grid #2: {{ }}2(a),(c) Grid #3: {{ }}2(a),(c) Grid #4: {{ }}2(a),(c)
{{ }}2(a),(c),ECI	{{ }}2(a),(c) {{ }}2(a),(c) {{ }}2(a),(c) {{ }}2(a),(c) {{ }}2(a),(c) {{ }}2(a),(c)

[7] Only spacer grids {{ }}2(a),(c) are modeled in VIPRE-01

{{

}}2(a),(c),ECI

Figure 3-15. KATHY NuFuel-HTP2™ K9300 test section schematic

NuScale Nonproprietary

3.1.2.6 AREVA Test Loop

The AREVA KATHY test facility, has been in operation since 1986 and can be used for a variety of thermal-hydraulic tests for pressurized water and boiling water reactors. The KATHY test loop is illustrated in Figure 3-16 and its design conditions are tabulated in Table 3-11. The PWR test loop is utilized for the NuFuel-HTP2™ CHF tests.

The KATHY loop's 300 kW pressurizer has a volume of 1.0 m^3 and a design pressure and temperature consistent with the test vessel. The circulation pump has a design maximum pressure of 210 bar (3046 psia) and a design maximum temperature of 370 degrees Celsius (698 degrees Fahrenheit). The loop's electric power supply has a maximum (gross) power of 20 MW and a maximum current of 80 kA at 230V.

[

].

Table 3-11. KATHY loop design conditions

Parameter	Value
Design pressure	185 bar (2683 psia)
Design temperature	360 °C (680 °F)

NuScale Nonproprietary

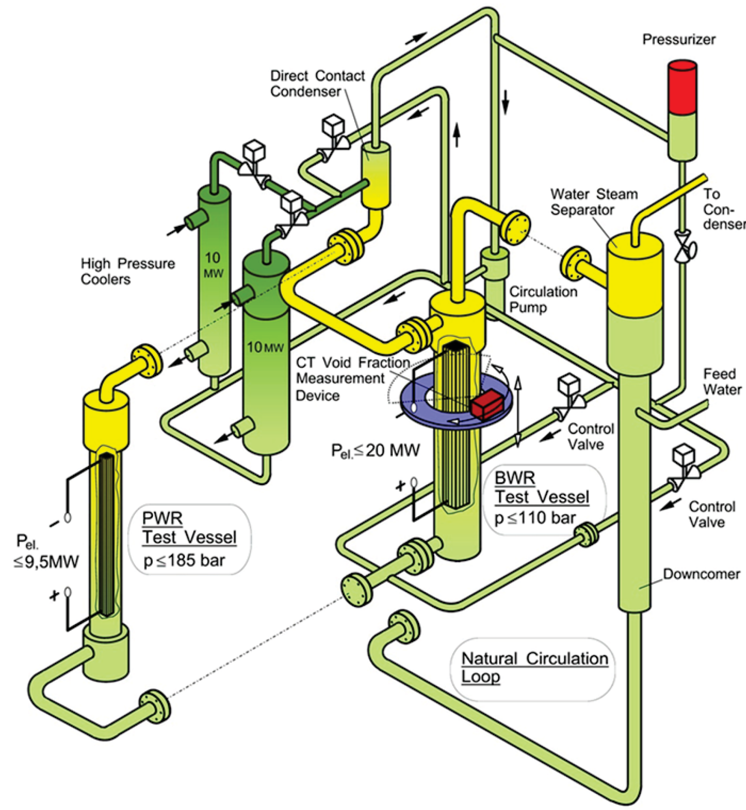

Figure 3-16. AREVA's KATHY facility layout

3.1.2.7 AREVA Instrumentation and Data Acquisition System

The test section and loop are instrumented to measure power, flow rates, absolute pressures, and coolant and fuel simulator temperatures during testing. System pressure is measured by two pressure transducers at the outlet of the test section (flow channel). The inlet temperature is measured at the test vessel inlet by two independent, calibrated RTDs. The outlet temperature is measured by three RTDs. The flow is determined using the measured pressure drop across the orifices using a pressure transducer. All measurement devices used during the experiments were in current calibration.

[

]. The installed heater rod thermocouples are checked for acceptable operation prior to the heater rod installation into the test bundle.

Two independent and diverse methods are applied to measure the electric current through the test bundle: the first is based on the Faraday effect and, the second is based on four high precision fast response shunts. At least one heater rod is equipped with voltage taps across the heated length. This measurement is used to determine the electric power to the test bundle. The voltage between the busbars is also measured as

a backup measurement. The measured current and voltage is used to calculate the total bundle power.

The DAS is used to scan the instrumentation and convert the signals to engineering units and perform calculations. A list of the primary DAS variables and their associated uncertainties are tabulated in Table 3-12. Analog signals of the loop instrumentation are sampled by digital converter and stored to hard disk at a sampling rate per channel of 20 Hz. All data from the test run are retained and available for engineering assessment. Select data channels are displayed on a bank of three displays with particular attention paid to visualization of the **[ ]**. The evaluation software transfers the measured values into physical values (e.g., pressure, temperature and mass flow rate).

During testing, power is slowly ramped when approaching CHF. A CHF event is characterized by an increase in the measured temperatures of thermocouples positioned inside the heater rods. **[ ]** are used to check for the occurrence of onset of CHF: **[ ]**. Two "reference points" are selected to allow a more efficient transition from anywhere in the testing range to a nearby "reference point" to determine if the measured performance level is maintained for the test bundle and loop operation. Periodically the test loop is taken back to one of the "reference points" to verify integrity of the test bundle. A check is repeated during the test series each day or if there are any indications of abnormalities in testing. The test repeatability at these "reference points" is acceptable and is within past testing experience.

During CHF testing, loop stability is controlled by monitoring the pressure, inlet flow and inlet temperature. Nominal values for these three parameters for each statepoint are prescribed and the values are not allowed to deviate from the nominal values beyond the ranges specified in Table 3-13. During the test run the parameter values are not allowed **[ ]** specified in Table 3-13. During the last **[ ]** prior to CHF the **[ ]** specified in Table 3-13. This graded approach to assuring loop stability is illustrated in Figure 3-17.

The test loop heat loss is the amount of energy lost from the test vessel that does not contribute to the enthalpy increase of the fluid flowing through the test channel. Heat losses have been characterized at KATHY and concluded to be **[ ]**. This value is accounted for in the validation of the NSP2 CHF correlation.

Table 3-12. KATHY DAS variables and estimated uncertainties

Variable	Uncertainty
System pressure	**[ ]**
Mass flux	**[ ]** **[ ]**
Inlet temperature	**[ ]**
Bundle Power	**[ ]**

NuScale Nonproprietary

Table 3-13. KATHY maximum deviations of CHF test parameters

Parameter	Pressure	Inlet Mass Flux	Inlet Temperature
Max. deviation from nominal value	[ ]	[ ] [ ]	[ ]ECI
Max. deviation from [ ]	[ ]	[ ] [ ] [ ]	[ ]ECI
Max. deviation from [ ]	[ ]	[ ] [ ] [ ]	[ ]ECI

[

]

Figure 3-17. Monitoring of loop stability during CHF testing

3.2 Statistical Evaluation Methods

The following sections describe the statistical methods employed in the development of the NSP2 CHF correlation. In order to meet the regulatory criteria outlined in Section 2.1 CHF must be avoided at the 95/95 level, which implies a required level of significance, α, of 0.05. Therefore, the level of significance is considered to be 0.05 for all statistical processes involved in the development of the NSP2 CHF correlation.

3.2.1 Treatment of Outliers

An outlier is considered to be an "apparently erroneous observation that has been identified by some statistical procedure as due to error or some cause rather than

randomness in the data" (refer to Reference 8.2.1, Section 26.2). In the traditional sense, an outlier would tend to be measured data, such as a test measurement, that could be affected by unknown outside influences. When this concept is applied to a correlation of data, which is a mathematical rather than physical process, external factors that are spurious in nature are excluded. While it is possible to justify the removal of outliers from a correlation in this manner, this is not the approach employed in the development or assessment of the NSP2 CHF correlation. The methodology encompasses the complete population of constituent data and the uncertainty of the correlation in its entirety in deriving the correlation limit.

3.2.2 Critical Heat Flux Test Uncertainties

The measured test values of bundle inlet temperature, average mass flux, pressure, and power are used as boundary conditions for determining {{ }}[2(a),(c)] for each CHF statepoint tested. The overall test uncertainty, including measurement and repeatability uncertainties, is included in this measured test data based on the premise that sufficient test data are taken such that the standard deviation or cumulative distribution function of the measured-to-predicted ratio (M/P) values encompass these uncertainties. Therefore, the CHF correlation limit accounts for these uncertainties. Furthermore, system biases and uncertainties are applied in the subchannel methodology to conservatively account for plant uncertainties associated with these same parameters, which are of the same order of magnitude as the CHF test uncertainties.

3.2.3 Tests for Normality

It is important to establish whether a particular population may be considered to be from a normal distribution, because this test determines whether to employ parametric or non-parametric statistical methods. One of two statistical normality tests is applied to test whether a population belongs to a normal distribution:

1. Shapiro-Wilks' *W*-test if there are fifty (50) or less data (Reference 8.2.1, Section 11.9), or

2. D'Agostino's D' test if there are more than fifty (50) data (Reference 8.2.1, Section 11.10).

3.2.4 Comparisons of Data Sets

The complete data set is {{

}}2(a),(c).

For parametric data, the Bartlett test of homoscedasticity (Reference 8.2.1, Section 14.7) is performed on data subsets to test whether the variances are considered equal. For non-parametric data, the k-Sample Squared Ranks test (Reference 8.2.1, Section 25.14) is performed to test equality of variances. If the null hypothesis that the variances are equal is rejected, then the median test of locations (Reference 8.2.1, Section 25.9) is used to determine whether data subsets can be combined. Otherwise, the Kruskal-Wallis test of locations (Reference 8.2.1, Section 25.10) is used because the Kruskal-Wallis test assumes that variances are equal. If it can be statistically shown that data subsets have equal means then they are combined into larger data groups. When combining data into groups it is possible that some data subsets can belong to multiple groups. For example, consider a simple case with three subsets: α, β, and γ; it is possible that α can be combined with β, and γ, but that β cannot be combined with γ. In this case α, β, and γ cannot be combined into a single group, but α can be combined with β to make one group and α can be combined with γ to make a second group.

3.2.5 Correlation Limit

The CHF correlation limit is equivalent to a one-sided tolerance limit of the predicted-to-measured ratio (P/M) CHF values. If the P/M sample can be shown to belong to a normal distribution then a parametric statistical tolerance limit method (Reference 8.2.1; §9.12) is used. If the sample cannot be shown to belong to the normal distribution then a non-parametric statistical tolerance limit method using order statistics is used. If a random sample n is taken from a population having a continuous distribution function $F(x)$ the samples are ordered ascendingly as $x_1, x_2, \ldots, x_i, \ldots, x_n$, as illustrated in Figure 3-18. The fraction β of the population that lie between the i^{th} and j^{th} values (i.e., x_i and x_j) in the sample is $F(x_j) - F(x_i)$. This quantity is referred to as the population coverage of the interval (x_i, x_j) and has the probability element:

$$\frac{\Gamma(n+1)}{\Gamma(k)\Gamma(n-k+1)}\, u^{k-1}(1-u)^{n-k}du \qquad \text{Eq. 3-2}$$

where u is the probability of the statistic falling in the interval. The probability α that the coverage is at least β is given as:

$$\alpha = \int_{\beta}^{1} \frac{\Gamma(n+1)}{\Gamma(k)\Gamma(n-k+1)} u^{k-1}(1-u)^{n-k}du \qquad \text{Eq. 3-3}$$

where $k = n - j + i$ and α is referred to as the tolerance level. The above equation is simplified and the value of k is maximized so that:

$$\alpha \leq 1 - I_{\beta}(n-k+1, \mathrm{k}) \qquad \text{Eq. 3-4}$$

Where $I_x(A, B)$ is the incomplete beta distribution:

$$I_x(A,B) = \frac{\Gamma(A+B)}{\Gamma(A)\Gamma(B)} \int_0^x z^{A-1}(1-z)^{B-1}\, dz, \qquad \text{Eq. 3-5}$$

For all variations of A and B the following equality holds:

$$I_{1-\beta}(k, n-k+1) = 1 - I_{\beta}(n-k+1, k) \qquad \text{Eq. 3-6}$$

Therefore, Eq. 3-3 can be expressed as:

$$\alpha \leq I_{1-\beta}(k, n-k+1) \qquad \text{Eq. 3-7}$$

Tolerance limits are calculated for each data subset grouping discussed in Section 3.2.4. The maximum tolerance limit for all of the groups is adopted as the correlation limit, because this limit conservatively bounds all of the groups.

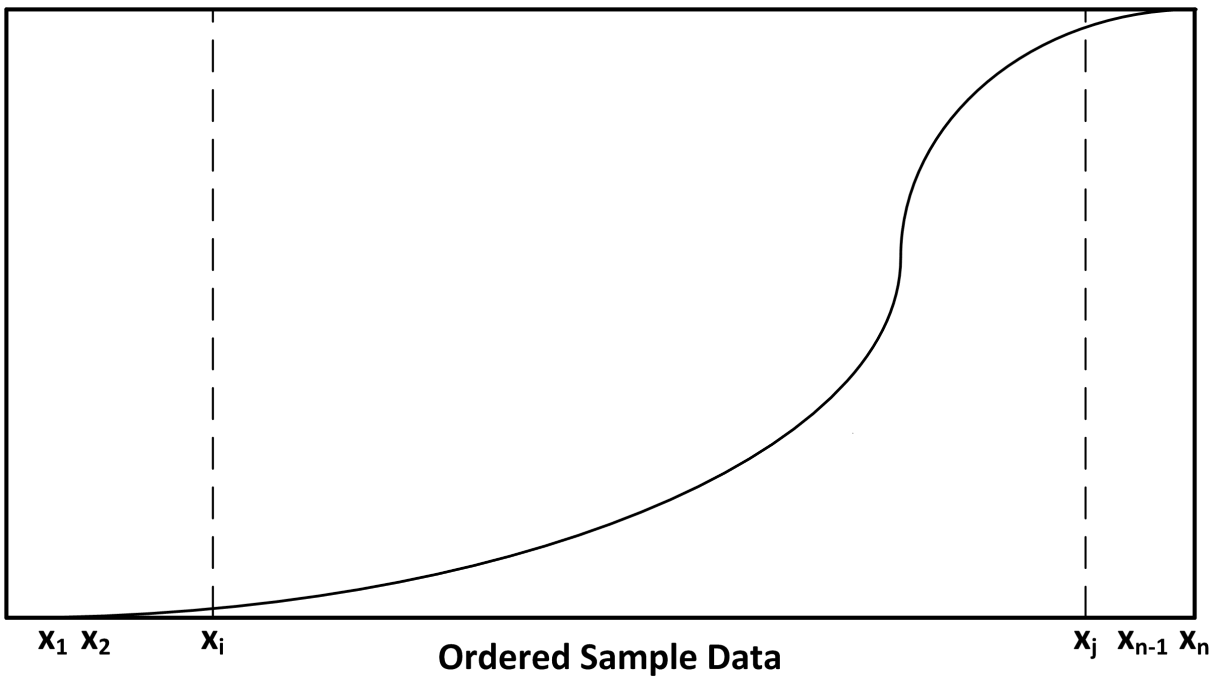

Figure 3-18. Illustrative non-parametric probability distribution function

3.3 Local Conditions

The CHF test data provide global parameter values such as system pressure, inlet temperature, and total bundle power. The NSP2 CHF correlation, however, is based on thermal-hydraulic conditions {{ }}$^{2(a),(c)}$. These parameters include, but are not limited to, {{ }}$^{2(a),(c)}$. The {{ }}$^{2(a),(c)}$. The following sections describe the generic and test specific modeling options selected.

3.3.1 VIPRE-01 Models

The radial geometry of the Stern preliminary prototypic U1, U2 and C1 tests is represented by a 36-channel model of the test assembly in full radial detail, as illustrated in Figure 3-4 for the U1 and C1 tests and Figure 3-5 for the U2 test. The model represents the heated length of the test section with grid spacers represented with discrete nodes to capture the diversion crossflow at appropriate locations. Maximum axial node size is {{ }}$^{2(a),(c)}$ The {{ }}$^{2(a),(c),ECI}$ for the U1 and U2 tests and {{ }}$^{2(a),(c)}$ for the C1 test, as discussed in Section 3.1.1.1. The {{ }}$^{2(a),(c)}$ of C1 is defined by Eq. 3-1. Operating conditions are based on the measured exit pressure, inlet temperature, inlet mass flux, and average linear heat generation rate, which vary for each test point.

NuScale Nonproprietary

The radial geometry of the KATHY K8500 HMP™ and KATHY NuFuel-HTP2™ K9000, K9100, K9200, and K9300 tests are also represented by similar 36-channel models of the test assembly in full radial detail. The models cover the heated length of the test section with spacer grids represented with discrete nodes. Maximum axial node size for any of the KATHY models is {{ }}2(a),(c) The {{ }}2(a),(c),ECI for the **[ ]** tests, and {{ }}2(a),(c),ECI for the **[ ]** tests. Operating conditions are based on the measured exit pressure, inlet temperature, inlet mass flux, and average linear heat generation rate, which vary for each test point.

Each of the VIPRE-01 models, for the Stern preliminary prototypic, KATHY K8500 HMP™ and KATHY NuFuel-HTP2™ tests, use the same VIPRE-01 two-phase, heat transfer and mixing correlation inputs. The two-phase and heat transfer correlation models are tabulated in Table 3-14 and the mixing models are tabulated in Table 3-15. The models in these two tables are identical to those identified for safety analysis of the NPM per the subchannel analysis methodology topical report (Reference 8.2.3). Justification for the selection of these models is discussed in the subchannel analysis methodology topical report (Reference 8.2.3). Therefore, the two-phase and heat transfer correlations listed in Table 3-14 and Table 3-15 must be used in any safety analysis of the NPM that utilizes the NSP2 CHF correlation.

Table 3-14. Two-phase and heat transfer correlations

Correlation	VIPRE-01 Model	Notes
Two-phase friction multiplier	EPRI	The EPRI correlations are recommend in the guidelines for two-phase models because they provided the best overall benchmark to data. (VIPRE-01 default option)
Two-phase subcooled void	EPRI	
Two-phase bulk void	EPRI	
Hot wall friction correction	NONE	
Single-phase forced convection heat transfer	EPRI	The EPRI correlation is the Dittus-Boelter correlation with the leading coefficients defined to correspond to the EPRI void models (VIPRE-01 default option)
Subcooled boiling heat transfer	THSP	The Thom correlation (VIPRE-01 default option)
Saturated boiling heat transfer	THSP	The Thom correlation (VIPRE-01 default option)
Transition boiling heat transfer	COND	The Condie-Bengtson correlation (VIPRE-01 default option)
Film boiling heat transfer	G5.7	The Groeneveld 5.7 correlation (VIPRE-01 default option)

Table 3-15. Turbulent mixing factors

Correlation	Value	Notes
Turbulent momentum factor	0.8	This is the default recommended value for VIPRE-01 and it has been determined that the sensitivity of this parameter ranging from 0 to 1 is negligible
Single-phase mixing coefficient correlation	$w' = \beta S\bar{G}$	Use a standard Rowe & Angle type model
β value	{{ }}2(a),(c),ECI	Based on single-phase data from Stern Laboratories thermal mixing tests
Two-phase mixing coefficient correlation	-	Treated the same as single-phase mixing, which has been found to be conservative

3.3.2 VIPRE-01 Data Reduction

VIPRE-01 {{ }}2(a),(c). For the Stern preliminary prototypic tests, {{ }}2(a),(c). The [ ]. Local conditions for KATHY NuFuel-HTP2™ K9000 through K9300 are {{ }}2(a),(c). These data are used to validate the NSP2 CHF correlation. Using {{ }}2(a),(c). Higher P/M values are more challenging relative to validating that the NSP2 CHF correlation can conservatively predict NuFuel-HTP2™ fuel CHF. Therefore, the NSP2 CHF correlation can be shown to provide conservative predictions of CHF for the KATHY NuFuel-HTP2™ data without concerns that there are other more challenging local thermal-hydraulic conditions.

The local conditions obtained from VIPRE-01 include:

- {{ }}2(a),(c)
- {{ }}2(a),(c)

Global parameters obtained from VIPRE-01 include:

- {{ }}2(a),(c)
- saturated liquid enthalpy, Btu/lbm
- saturated vapor enthalpy, Btu/lbm

Other parameters considered for the CHF development include:

- {{ }}2(a),(c)
- {{ }}2(a),(c)
- {{ }}2(a),(c)
- {{ }}2(a),(c)
- {{ }}2(a),(c)
- {{ }}2(a),(c)
- {{ }}2(a),(c)
- {{ }}2(a),(c)
- {{ }}2(a),(c)

All of these parameters are considered in one way or another for the base CHF correlation. For reference, the primary parameters common to most CHF correlations are pressure, local mass flux, and local quality.

4.0 Base Critical Heat Flux Correlation Development

The base CHF correlation is based upon Stern preliminary prototypical CHF test data. This data meets general behavioral expectations. The measured uniform CHF is found to {{

}}[2(a),(b),(c)]. Therefore, the trends in Figure 4-1 are consistent with expectations considering the combined effect of {{ }}[2(a),(c)]. This trend is consistent with that of the KATHY K8500 HMP™ data in Figure 5-1. The linear fit of the data demonstrates a trend of {{ }}[2(a),(b),(c)], as illustrated in Figure 4-2. This trend meets expectations, as the {{ }}[2(a),(c)] aid in the removal of heat from the heater rods. Also, the linear fit of the data demonstrate a trend of {{ }}[2(a),(b),(c)], as illustrated in Figure 4-3. This trend meets expectations, as the {{ }}[2(a),(b),(c)] that inhibits heat removal from the heater rods.

{{

}}[2(a),(b),(c)]

Figure 4-1. Measured uniform CHF vs. pressure (Stern preliminary prototypic)

{{

}}2(a),(b),(c)

Figure 4-2. Measured uniform CHF vs. local mass flux (Stern preliminary prototypic)

{{

}}2(a),(b),(c)

Figure 4-3. Measured uniform CHF vs. local quality (Stern preliminary prototypic)

4.1 Correlating Technique

The ultimate goal of the CHF correlation is to provide a tool to predict CHF for safety analysis and provide a correlation limit that assures the guidance given by acceptance criterion 1 of Reference 8.1.3 is met. The Stern preliminary prototypic tests encompass a range of thermal-hydraulic conditions necessary to establish the CHF-based safety analysis protection measures for the NPM, but do not provide a continuous database where all applicable operating conditions are included. A {{ }}[2(a),(c)] process is employed to optimize and validate the final correlation. A {{ }}[2(a),(c)] is employed in evaluating the base CHF correlation. {{ }}[2(a),(c)]. The complete data population (all local condition data) is {{ }}[2(a),(c)]. The correlation coefficients derived from {{ }}[2(a),(c)] to produce the final correlation coefficients. The coefficients and statistical results of {{ }}[2(a),(c)] predicts similar values. The coefficients and statistical results are also determined for the full data set and compared to the results {{ }}[2(a),(c)].

4.2 Correlation Form

The base CHF correlation is determined using an additive linear least squares regression. The linear terms include the following:

- {{ }}[2(a),(c)]
- {{ }}[2(a),(c)]
- {{ }}[2(a),(c)]
- {{ }}[2(a),(c)]
- {{ }}[2(a),(c)]
- {{ }}[2(a),(c)]

The {{ }}[2(a),(c)] is defined by:

{{

Eq. 4-1

}}[2(a),(c)]

NuScale Nonproprietary

where,

{{ }}2(a),(c)

{{ }}2(a),(c)

{{ }}2(a),(c)

The {{ }}2(a),(c).

The {{ }}2(a),(c).

{{ }}2(a),(c). Through this process, the base CHF correlation is found to have the form:

{{ Eq. 4-2 }}2(a),(c)

The critical heat flux ratio (CHFR) is defined as:

$$CHFR = q''_{C,u}/(q''_L \times FNU) \quad \text{Eq. 4-3}$$

where,

{{ }}2(a),(c)

{{ }}2(a),(c)

{{ }}2(a),(c)

{{ }}2(a),(c)

{{ }}2(a),(c)

{{ }}2(a),(c)

$q''_{C,u}$ = uniform CHF, 10^6 Btu/hr-ft^2

q''_L = local heat flux, 10^6 Btu/hr-ft^2

P = pressure, psia

NuScale Nonproprietary

{{ }}^2(a),(c)

G = local mass flux, 10^6 lbm/hr-ft^2

X = local equilibrium quality

{{ }}^2(a),(c)

{{ }}^2(a),(c)

{{ }}^2(a),(c)

{{ }}^2(a),(c)

{{ }}^2(a),(c)

FNU = non-uniform flux factor discussed in Section 4.3

c_x = CHF correlation coefficients (see Table 4-1)

Table 4-1. Base CHF correlation coefficients

Coefficient	Value	Coefficient	Value
c_0	{{ }}^2(a),(c)	c_8	{{ }}^2(a),(c)
c_1	{{ }}^2(a),(c)	c_9	{{ }}^2(a),(c)
c_2	{{ }}^2(a),(c)	c_{10}	{{ }}^2(a),(c)
c_3	{{ }}^2(a),(c)	c_{11}	{{ }}^2(a),(c)
c_4	{{ }}^2(a),(c)	c_{12}	{{ }}^2(a),(c)
c_5	{{ }}^2(a),(c)	c_{13}	{{ }}^2(a),(c)
c_6	{{ }}^2(a),(c)	c_{14}	{{ }}^2(a),(c)
c_7	{{ }}^2(a),(c)	c_{15}	{{ }}^2(a),(c)

4.3 Non-Uniform Flux Factor Development

An FNU, Tong (Reference 8.2.4), is used to adjust CHF predictions for the effect of variations of axial power profiles. The Tong FNU is based on a wide variety of axial power shapes and has been previously employed to account for axial power shape variations. The Tong FNU is given as:

$$FNU = \frac{C\int_0^{l_{CHF}} q''(z)e^{-C(l_{CHF}-z)}dz}{q''_{(l_{CHF})} \times (1 - e^{-C\cdot l_{CHF}})} \qquad \text{Eq. 4-4}$$

where,

{{ }}^2(a),(c)

G = mass flux at CHF location, 10^6 Btu/hr-ft^2

l_{CHF} = elevation of CHF from bottom of heated length

NuScale Nonproprietary

$q''(z)$ = heat flux at elevation z, 10^6 Btu/hr-ft^2

$q''(l_{CHF})$ = heat flux at CHF location, 10^6 Btu/hr-ft^2

X = equilibrium quality at CHF location

This factor is applied to capture the effect of non-uniform axial power profiles as follows:

$$q''_{C,n} = q''_{C,u}/FNU \quad \text{Eq. 4-5}$$

where,

$q''_{C,u}$ = uniform CHF, 10^6 Btu/hr-ft^2

$q''_{C,n}$ = non-uniform heat flux, 10^6 Btu/hr-ft^2

FNU = Tong non-uniform flux factor

When the {{ }}$^{2(a),(c)}$ is necessary. By comparing the {{ }}$^{2(a),(c)}$, as depicted by Figure 4-4. Thus the FNU term is finally expressed as:

{{

Eq. 4-6

}}$^{2(a),(c)}$

The effect of applying this multiplier is illustrated in Figure 4-4.

{{

}}2(a),(b),(c)

Figure 4-4. Stern Preliminary Prototypic U1 and C1 CHF

4.4 Statistical Evaluation

The mean and root mean square error of the M/P CHF values for the {{ }}2(a),(c) are tabulated in Table 4-2. For the {{ }}2(a),(c), the mean M/P is within {{ }}2(a),(c) of unity, and using the {{ }}2(a),(c) results in a mean M/P of {{ }}2(a),(c), which represents a negligible bias. The root mean square error values fall within a range of {{ }}2(a),(c). The predicted versus measured heat flux values are illustrated in Figure 4-5. The majority of data falls along the ideal 45 degree line and {{ }}2(a),(c) of this ideal line. Biases with respect to the correlating parameters are evaluated by examining plots of M/P CHF versus each parameter. There is no distinct bias for any of the correlating parameters as illustrated in Figure 4-6 for pressure, Figure 4-7 for mass flux, Figure 4-8 for quality, Figure 4-9 for {{ }}2(a),(c), and Figure 4-10 for the {{ }}2(a),(c). With no distinct bias in M/P CHF values or with regards to the correlating parameters, the base CHF correlation predicts the Stern Laboratories test data in an acceptable manner.

Table 4-2. Base CHF correlation M/P mean and RMS error

Coefficient	Mean M/P CHF	M/P CHF Root Mean Square Error
{{ }}2(a),(c)	{{ }}2(a),(b),(c)	{{ }}2(a),(c)
{{ }}2(a),(c)	{{ }}2(a),(b),(c)	{{ }}2(a),(c)
{{ }}2(a),(c)	{{ }}2(a),(b),(c)	{{ }}2(a),(c)
{{ }}2(a),(c)	{{ }}2(a),(b),(c)	{{ }}2(a),(c)
{{ }}2(a),(c)	{{ }}2(a),(b),(c)	{{ }}2(a),(c)
{{ }}2(a),(c)	{{ }}2(a),(b),(c)	{{ }}2(a),(c)
Coefficients based on full data	{{ }}2(a),(b),(c)	{{ }}2(a),(c)

{{

}}2(a),(b),(c)

Figure 4-5. Predicted vs. measured CHF for Stern preliminary prototypic data

NuScale Nonproprietary

{{

}}2(a),(b),(c)

Figure 4-6. M/P CHF vs. pressure for Stern preliminary prototypic data

{{

}}2(a),(b),(c)

Figure 4-7. M/P CHF vs. local mass flux for Stern preliminary prototypic data

{{

}}2(a),(b),(c)

Figure 4-8. M/P CHF vs. local equilibrium quality for Stern preliminary prototypic data

{{

}}2(a),(b),(c)

Figure 4-9. M/P CHF vs. boiling length for Stern preliminary prototypic data

{{

}}[2(a),(b),(c)]

Figure 4-10. M/P CHF vs. cold wall factor for Stern preliminary prototypic data

4.5 Correlation Limit

While many discussions in this report are based on the M/P, when it comes to determining the correlation limit, the P/M is more appropriate. When considering the definition of CHFR, the CHF calculated with the correlation is the same whether being compared to test data or applied to safety analyses and the local heat flux in operation can be considered analogous to the measured heat flux from the CHF test. Thus:

$$CHFR = \frac{q''_{CHF}}{q''_{L}} \approx \frac{PREDICTED}{MEASURED} \qquad \text{Eq. 4-7}$$

The Stern preliminary prototypic data is {{ }}[2(a),(c)] as tabulated in Table 4-3. These {{ }}[2(a),(c)] from the Stern preliminary prototypic CHF test matrix (see Table 3-1) for {{ }}[2(a),(c)]. For {{ }}[2(a),(c)]. Tolerance limits, at the 95/95 level, for {{ }}[2(a),(c)] in Table 4-3 are calculated and tabulated in Table 4-4. The maximum tolerance limit is {{ }}[2(a),(c)]. Therefore, the base CHF correlation limit is found to be 1.17 to prevent CHF at the 95/95 level.

Table 4-3. Data subsets for Stern preliminary prototypic data

{{

}}2(a),(b),(c)

Table 4-4. Tolerance limits for Stern preliminary prototypic data

{{

}}2(a),(c)

4.6 Range of Applicability

The range of applicability in Table 4-5 is determined from the data points used in the development of the base CHF correlation. The values for the most significant parameters are tabulated in Table 4-5. The range of data listed covers the data at the 95/95 level (using non-parametric two-sided tolerance limit methods). There is no lower limit on local quality because the trends with regards to quality indicate reasonable and predictable behavior at low qualities.

Table 4-5. Parameter ranges of applicability for base CHF correlation

Parameter	Range of Applicability
pressure, psia	300 to 2300
local mass flux, 10^6 lbm/hr-ft^2	0.110 to 0.700
local equilibrium quality, %	≤ 95.0%

4.7 Base Correlation Performance

The performance of the base uniform CHF correlation is assessed with a global sensitivity analysis. A large set of statepoints {{ }}2(a),(c) are generated randomly within the ranges of the correlating parameters describing bundle boundary conditions. {{ }}2(a),(c) corresponding to these statepoints are randomly selected. The {{

}}2(a),(c). The predicted CHF {{ }}2(a),(b),(c), as illustrated in Figure 4-11, is consistent with the data trend established in Figure 4-1. The predicted CHF {{ }}2(a),(b),(c), as illustrated in Figure 4-12, is consistent with the data trend established in Figure 4-2. The predicted CHF {{ }}2(a),(b),(c), as illustrated in Figure 4-13, is consistent with the data trend established in Figure 4-3. Therefore, the base CHF correlation predicts CHF values in a manner that is consistent with the measured Stern preliminary prototypic data.

{{

}}2(a),(b),(c)

Figure 4-11. Global sensitivity – predicted uniform CHF vs. pressure

{{

}}2(a),(b),(c)

Figure 4-12. Global sensitivity – predicted uniform CHF vs. mass flux

{{

}}2(a),(b),(c)

Figure 4-13. Global sensitivity – predicted uniform CHF vs. quality

5.0 NSP2 Critical Heat Flux Correlation Development

5.1 Assessment of KATHY K8500 HMP™ Test with Base Critical Heat Flux Correlation

Stern preliminary prototypic CHF tests were designed specifically for the operating conditions needed to support the CHF-based safety analysis protection for the NPM using the VIPRE-01 code. The Stern preliminary prototypic tests used {{ }}2(a),(c), while the NuFuel-HTP2™ fuel design uses AREVA's HTP™ and HMP™ spacer grid technology. Data were obtained for fluid conditions similar to the Stern preliminary prototypic tests for a bundle of comparable geometry with HMP™ spacer grids from the KATHY K8500 HMP™ test. Comparisons of significant test parameters from the Stern preliminary prototypic and KATHY K8500 HMP™ tests are tabulated in Table 5-1. **[**

]. The grid spacers {{

}}2(a),(c). Therefore, the HTP™ grid spacer employed in the NuFuel-HTP2™ fuel design will produce {{ }}2(a),(c),ECI than either the Stern preliminary prototypic or KATHY K8500 HMP™ tests as it is designed to {{ }}2(a),(c),ECI. This conclusion is validated with testing of the NuFuel-HTP2™ fuel design as discussed in Section 6.0. The KATHY K8500 HMP™ local conditions fall within the Stern preliminary prototypic test local condition ranges for pressure, mass flux, and equilibrium quality, as illustrated in Figure 5-1 through Figure 5-3. **[**

].

The base correlation predictions of CHF values for KATHY K8500 HMP™ data are illustrated in Figure 5-4. {{

}}2(a),(c).

Table 5-1. Stern preliminary prototypic and KATHY K8500 HMP™ parameters

Parameter	Stern Preliminary Prototypic	KATHY K8500 HMP™
Heater rod diameter, in.	{{ }}$^{2(a),(c)}$	[ ]
Heater rod pitch, in.	{{ }}$^{2(a),(c),ECI}$	[ ]^{ECI}
Channel width, in.	{{ }}$^{2(a),(c),ECI}$	[ ]^{ECI}
Heated length, in.	{{ }}$^{2(a),(c),ECI}$	[ ]^{ECI}
Grid spacer design	{{ }}$^{2(a),(c)}$	HMP™
Distance between grid spacers, in.	{{ }}$^{2(a),(c)}$	[ ]
Radial powers (max/min)	{{ }}$^{2(a),(c)}$	[ ]
Axial power profile	{{ }}$^{2(a),(c),ECI}$	[ ]^{ECI}
Average mass flux, 10^6 lbm/hr-ft^2	{{ }}$^{2(a),(c)}$	[ ]
Pressure, psia	{{ }}$^{2(a),(c)}$	[ ]
Local quality	{{ }}$^{2(a),(c)}$	[ ]

{{

}}$^{2(a),(b),(c)}$

Figure 5-1. CHF vs. pressure for Stern preliminary prototypic and KATHY K8500 HMP™

{{

}}2(a),(b),(c)

Figure 5-2. CHF vs. mass flux for Stern preliminary prototypic and KATHY K8500 HMP™

{{

}}2(a),(b),(c)

Figure 5-3. CHF vs. quality for Stern preliminary prototypic and KATHY K8500 HMP™

{{

}}2(a),(b),(c)

Figure 5-4. Base P/M CHF for Stern preliminary prototypic and KATHY K8500 HMP™

5.2 NSPX factor for HMP™ and HTP™ Fuel

The NSPX factor is used to {{ }}2(a),(c) of the KATHY K8500 HMP™ data. {{

}}2(a),(c). The NSPX factor has the form:

{{

Eq. 5-1

}}2(a),(c)

{{

}}2(a),(b),(c)

Figure 5-5. Base CHF Correlation M/P CHF vs. pressure for KATHY K8500 HMP™

5.3 NSP2 Critical Heat Flux Correlation

The NSP2 CHF correlation combines the CHF prediction of the base CHF correlation with the NSPX factor:

{{

Eq. 5-2

}}2(a),(c)

where,

$q''_{C,u}$ = uniform CHF from base correlation, 10^6 Btu/hr-ft^2

F_{NuFuel} = NSPX factor

{{ }}2(a),(c)

{{ }}2(a),(c)

{{ }}2(a),(c)

NuScale Nonproprietary

{{ }}2(a),(c)

{{ }}2(a),(c)

{{ }}2(a),(c)

P = pressure, psia

{{ }}2(a),(c)

G = local mass flux, 10^6 lbm/hr-ft^2

X = local equilibrium quality

{{ }}2(a),(c)

{{ }}2(a),(c)

{{ }}2(a),(c)

{{ }}2(a),(c)

{{ }}2(a),(c)

c_x = CHF correlation coefficients (see Table 4-1)

The effect of the NSPX factor is illustrated with the M/P heat flux values for both the base and final NSP2 CHF correlations in Figure 5-6. With the NSPX factor applied, the KATHY K8500 HMP™ and Stern preliminary prototypic data are conservatively predicted.

{{

}}2(a),(b),(c)

Figure 5-6. Base and NSP2 predicted vs. measured CHF for KATHY K8500 HMP™

6.0 Validation with NuFuel-HTP2™ Fuel Design

The NSP2 correlation is developed using test data from test bundles that are geometrically comparable, but have different spacer grids than the NuFuel-HTP2™ design that will be used for the NuScale DCA. Therefore, it is imperative to validate that the correlation adequately predicts CHF performance for the NuFuel-HTP2™ design that will be used in the NPM. In order to validate the correlation, the following are considered:

- Compare raw test data between Stern preliminary prototypic and KATHY NuFuel-HTP2™ tests.
- Predict CHF for KATHY NuFuel-HTP2™ test data with the NSP2 correlation and verify that it is conservatively predicted.
- Determine the applicable tolerance limit for the KATHY NuFuel-HTP2™ P/M data assuring that the correlation limit determined for the base CHF correlation (Section 4.5) remains conservative, or determining a more conservative limit specific to the KATHY NuFuel-HTP2™ data.

The KATHY NuFuel-HTP2™ data are from a test bundle design consistent with the NuFuel-HTP2™ fuel bundle considered in the NuScale DCA. The KATHY NuFuel-HTP2™ data were obtained using HTP™ and HMP™ spacer grids and the grid spacing is consistent with the NuFuel-HTP2™ design considered in the NuScale DCA.

6.1 Comparison of Stern Preliminary Prototypic to KATHY NuFuel-HTP2™ Test Data

The test matrix for KATHY NuFuel-HTP2™ testing is designed to have some direct overlap with the conditions tested with the Stern preliminary prototypic bundle design, so that comparisons can be made between data from the two designs. This approach accounts for {{ }}$^{2(a),(c)}$. Overlap with regards to {{ }}$^{2(a),(c)}$ and with regards to {{ }}$^{2(a),(c)}$ (refer to Table 3-1 and Table 3-4). Comparisons for the K9000, K9100, and K9300 tests are addressed in the following sections.

6.1.1 KATHY NuFuel-HTP2™ K9000 versus Stern Preliminary Prototypic U2

Data from KATHY NuFuel-HTP2™ K9000 and Stern preliminary prototypical U2 tests are compared qualitatively by plotting the measured hot rod average heat flux as a function of test matrix mass flux for the corresponding levels of test matrix inlet subcooling in Figure 6-1 through Figure 6-4. {{

}}2(a),(c) as described in Section 5.1.

Note: The y-axis values are omitted in Figure 6-1 through Figure 6-4 due to NuScale requirements for the handling of proprietary test data. All four plots use an identical y-axis range.

{{

}}2(a),(b),(c)

Figure 6-1. U2 vs. K9000 measured heat flux at 7.0 MPa

{{

}}2(a),(b),(c)

Figure 6-2. U2 vs. K9000 measured heat flux at 10.0 MPa

{{

}}2(a),(b),(c)

Figure 6-3. U2 vs. K9000 measured heat flux at 13.0 MPa

{{

}}2(a),(b),(c)

Figure 6-4. U2 vs. K9000 measured heat flux at 16.0 MPa

6.1.2 KATHY NuFuel-HTP2™ K9100 versus Stern Preliminary Prototypic U1

Data from KATHY NuFuel-HTP2™ K9100 and Stern preliminary prototypical U1 tests are compared qualitatively by plotting the measured hot rod average heat flux as a function of test matrix mass flux for corresponding levels of test matrix inlet subcooling in Figure 6-5 through Figure 6-8. {{

}}2(a),(c).

Note: The y-axis values are omitted in Figure 6-5 through Figure 6-8 due to NuScale requirements for the handling of proprietary test data. All four plots use an identical y-axis range.

{{

}}2(a),(b),(c)

Figure 6-5. U1 vs. K9100 measured heat flux at 7.0 MPa

{{

}}2(a),(b),(c)

Figure 6-6. U1 vs. K9100 measured heat flux at 10.0 MPa

{{

}}2(a),(b),(c)

Figure 6-7. U1 vs. K9100 measured heat flux at 13.0 MPa

{{

}}2(a),(b),(c)

Figure 6-8. U1 vs. K9100 measured heat flux at 16.0 MPa

6.1.3 KATHY NuFuel-HTP2™ K9300 versus Stern Preliminary Prototypic C1

Data from KATHY NuFuel-HTP2™ K9300 and Stern preliminary prototypical C1 tests are compared qualitatively by plotting the hot rod average heat flux as a function of test matrix mass flux for corresponding levels of test matrix inlet subcooling in Figure 6-9 through Figure 6-12. {{

}}2(a),(c).

Note: The y-axis values are omitted in Figure 6-9 through Figure 6-12 due to NuScale requirements for the handling of proprietary test data. All four plots use an identical y-axis range.

{{

}}2(a),(b),(c)

Figure 6-9. C1 vs. K9300 measured heat flux at 7.0 MPa

{{

}}2(a),(b),(c)

Figure 6-10. C1 vs. K9300 measured heat flux at 10.0 MPa

{{

}}2(a),(b),(c)

Figure 6-11. C1 vs. K9300 measured heat flux at 13.0 MPa

{{

}}2(a),(b),(c)

Figure 6-12. C1 vs. K9300 measured heat flux at 16.0 MPa

6.1.4 Summary of KATHY to Stern Laboratories Comparisons

Comparisons between Stern preliminary prototypic and KATHY NuFuel-HTP2™ data demonstrate that the NuFuel-HTP2™ assembly design performs {{ }}2(a),(c) with regards to CHF. The measured CHF for the KATHY NuFuel-HTP2™ test is, {{ }}2(a),(c). The trend demonstrated by Figure 6-1 through Figure 6-12 is expected because the HTP™ spacer grid {{ }}2(a),(c). Overall, the {{ }}2(a),(c) and supports the use of the KATHY NuFuel-HTP2™ data as a validation set for the NSP2 CHF correlation.

6.2 NuFuel-HTP2™ Critical Heat Flux Predictions with NSP2 Critical Heat Flux Correlation

The NSP2 CHF correlation predicts conservative CHF values for the NuFuel-HTP2™ design as demonstrated {{

}}2(a),(b)(c).

This conclusion is also demonstrated by the statistical mean values of P/M CHF for the four tests, which are {{ }}2(a),(b),(c). In Figure 6-14 {{

}}2(a),(b),(c). These results do not diminish the overall conservatism of the method, because the P/M CHF values that are above 1.0 are addressed by the final CHF correlation limit. {{

}}2(a),(b),(c).

{{

}}2(a),(b),(c)

Figure 6-13. NSP2 P/M CHF for KATHY NuFuel-HTP2™ tests

NuScale Nonproprietary

{{

}}2(a),(b),(c)

Figure 6-14. NSP2 P/M CHF for KATHY NuFuel-HTP2™ mass flux ranges

6.3 Correlation Limit for NuFuel-HTP2™

In order to develop a CHF correlation limit that meets regulatory requirements across the correlation applicability range, the CHF data is {{

}}2(a),(c). Tolerance limits, at the 95/95 level, for {{

}}2(a),(c). Furthermore, {{

}}2(a),(c). Therefore, the NSP2 CHF correlation limit is 1.17, which is conservative, to prevent CHF at the 95/95 level.

Table 6-1. Data subsets for KATHY NuFuel-HTP2™ data

{{

}}2(a),(b),(c)

Table 6-2. Tolerance limits for subset groupings of KATHY NuFuel-HTP2™ data

{{

}}2(a),(c)

6.4 Validation Conclusions

Comparison between KATHY NuFuel-HTP2™ and Stern preliminary prototypic test data demonstrates that the NuFuel-HTP2™ design has **[ ]**. For the majority of points the KATHY NuFuel-HTP2™ measured CHF values **[ ]** comparable Stern preliminary prototypic values. {{ }}2(a),(c).

All non-conservative predictions are conservatively addressed by appropriately setting the CHF correlation limit, which ensures that CHF will not be experienced by the limiting fuel rod at the 95/95 level. The correlation limit determined for sub-regions of the KATHY NuFuel-HTP2™ test data (refer to Section 6.3) is {{ }}2(a),(c) determined for the base CHF correlation. Therefore, the NSP2 CHF correlation is found to conservatively predict CHF for the NuFuel-HTP2™ fuel design and the correlation limit determined for the base CHF correlation (1.17) is applicable.

7.0 Summary and Conclusions

The CHF tests for NuScale were conducted at Stern Laboratories and at AREVA's KATHY test facility to obtain steady-state CHF data used in the derivation and validation of the NSP2 CHF correlation used for NPM safety analysis involving the NuFuel-HTP2™ fuel design.

The NSP2 CHF correlation is developed in two parts. The base CHF correlation is developed using the data from Stern Laboratories for {{ }}$^{2(a),(c)}$. These data encompass the operating range of the NPM that will be analyzed with the VIPRE-01 code for the NuScale DCA. An NSPX factor is separately developed from data obtained from existing KATHY testing {{ }}$^{2(a),(c)}$. The NSPX factor conservatively adjusts the base correlation such that it {{ }}$^{2(a),(c)}$. The combination of the base CHF correlation and the NSPX factor forms the basis for the NSP2 CHF correlation that will be used for safety analysis performed in support of the NuScale DCA. The NSP2 CHF correlation has the form:

{{

Eq. 7-1

}}$^{2(a),(c)}$

where,

{{ }}$^{2(a),(c)}$

{{ }}$^{2(a),(c)}$

{{ }}$^{2(a),(c)}$

{{ }}$^{2(a),(c)}$

{{ }}$^{2(a),(c)}$

{{ }}$^{2(a),(c)}$

$P =$ pressure, psia

{{ }}$^{2(a),(c)}$

$G =$ local mass flux, 10^6 lbm/hr-ft^2

$X =$ local equilibrium quality

{{ }}$^{2(a),(c)}$

{{ }}$^{2(a),(c)}$

{{ }}2(a),(c)

{{ }}2(a),(c)

{{ }}2(a),(c)

c_x = CHF correlation coefficients from regression (see Table 7-1)

Table 7-1. NSP2 CHF correlation coefficients

Coefficient	Value	Coefficient	Value
c_0	{{ }}2(a),(c)	c_8	{{ }}2(a),(c)
c_1	{{ }}2(a),(c)	c_9	{{ }}2(a),(c)
c_2	{{ }}2(a),(c)	c_{10}	{{ }}2(a),(c)
c_3	{{ }}2(a),(c)	c_{11}	{{ }}2(a),(c)
c_4	{{ }}2(a),(c)	c_{12}	{{ }}2(a),(c)
c_5	{{ }}2(a),(c)	c_{13}	{{ }}2(a),(c)
c_6	{{ }}2(a),(c)	c_{14}	{{ }}2(a),(c)
c_7	{{ }}2(a),(c)	c_{15}	{{ }}2(a),(c)

An FNU is used to account for the effect of non-uniform axial power profiles, and is defined as:

{{

Eq. 7-2

}}2(a),(c)

where,

{{ }}2(a),(c)

G = mass flux at CHF location, 10^6 Btu/hr-ft^2

l_{CHF} = elevation of CHF

$q''(z)$ = heat flux at elevation z, 10^6 Btu/hr-ft^2

$q''(l_{CHF})$ = heat flux at CHF location, 10^6 Btu/hr-ft^2

X = equilibrium quality at CHF location

The FNU is applied to convert the uniform NSP2 CHF to a non-uniform CHF with:

$$q''_{NSP2,n} = q''_{NSP2}/FNU \qquad \text{Eq. 7-3}$$

where,

q''_{NSP2} = uniform CHF, 10^6 Btu/hr-ft^2

$q''_{NSP2,n}$ = non-uniform heat flux, 10^6 Btu/hr-ft^2

$FNU =$ non-uniform flux factor

The NSP2 CHF correlation is validated against NuFuel-HTP2™ design specific CHF data obtained for NuScale at AREVA's KATHY test facility. The validation demonstrates that measured CHF values for KATHY NuFuel-HTP2™ data **[** **]** the Stern preliminary prototypic design for comparable operating conditions.

Evaluation of the NSP2 CHF correlation indicates that the correlation provides a conservative prediction **[** **]** KATHY NuFuel-HTP2™ test data. A correlation limit of 1.17 ensures at the 95/95 level that CHF will not be experienced on a rod demonstrating a limiting value, which meets acceptance criterion 1 of Reference 8.1.3 demonstrating compliance with the requirements of 10 CFR 50, GDC 10. The NSP2 CHF correlation must be used in conjunction with local condition calculations from the VIPRE-01 subchannel code (Reference 8.2.3). Qualification of VIPRE-01 for use in NPM calculations is outside of the scope of this report and is addressed in the NuScale Subchannel Analysis Methodology topical report (Reference 8.2.3). The ranges of applicability for the NSP2 CHF correlation are tabulated in Table 7-2.

NuScale requests NRC approval to use the NSP2 CHF correlation in VIPRE-01, within its range of applicability in Table 7-2, along with its associated correlation limit of 1.17, for the NuScale DCA and safety analysis of the NPM with NuFuel-HTP2™ fuel. This correlation conforms to acceptance criteria given by the NuScale DSRS, Section 4.4, and the requirements of 10 CFR 50, Appendix A, GDC 10.

Table 7-2. Parameter ranges of applicability for NSP2 CHF correlation

Parameter	**Range of Applicability**
pressure, psia	300 to 2300
local mass flux, 10^6 lbm/hr-ft^2	0.110 to 0.700
local equilibrium quality, %	≤ 95.0%

8.0 References

8.1 Source Documents

8.1.1 *U.S. Code of Federal Regulations*, “Appendix A to Part 50 – General Design Criteria for Nuclear Power Plants,” (10 CFR 50, Appendix A).

8.1.2 *U.S. Code of Federal Regulations*, “Part 50 – Domestic Licensing of Production and Utilization Facilities,” (10 CFR 50).

8.1.3 U.S. Nuclear Regulatory Commission, “Design-Specific Review Standard for NuScale SMR Design,” Section 4.4, June 2016.

8.1.4 NuScale Power, LLC, “Quality Assurance Program Description for the NuScale Power Plant,” TR-1010-859-NP, Rev. 3, March 2016, ML16084B004.

8.2 Referenced Documents

8.2.1 U.S. Nuclear Regulatory Commission, “Applying Statistics,” NUREG-1475, Rev.1, March 2011.

8.2.2 NuScale Power, LLC, "Critical Heat Flux Test Program Technical Report," TR-1113-5374, January 2014, Rev. 0, ML14024A452.

8.2.3 NuScale Power, LLC, "Subchannel Analysis Methodology," TR-0915-17564, Rev. 0, October 2016.

8.2.4 Tong, L.S., et. al., “Influence of Axially Non-uniform Heat Flux on DNB,” AIChE Chemical Engineering Progress Symposium, Series 62, (1966), 64:35-40.

Enclosure 3:

NuScale Affidavit, AF-0916-51388

NuScale Power, LLC
1100 NE Circle Blvd., Suite 200 Corvallis, Oregon 97330 Office 541.360-0500 Fax 541.207.3928
www.nuscalepower.com

NuScale Power, LLC

AFFIDAVIT of Thomas A. Bergman

I, Thomas A. Bergman , state as follows:

(1) I am the Vice President of Regulatory Affairs of NuScale Power, LLC (NuScale), and as such, I have been specifically delegated the function of reviewing the information described in this Affidavit that NuScale seeks to have withheld from public disclosure, and am authorized to apply for its withholding on behalf of NuScale

(2) I am knowledgeable of the criteria and procedures used by NuScale in designating information as a trade secret, privileged, or as confidential commercial or financial information. This request to withhold information from public disclosure is driven by one or more of the following:

(a) The information requested to be withheld reveals distinguishing aspects of a process (or component, structure, tool, method, etc.) whose use by NuScale competitors, without a license from NuScale, would constitute a competitive economic disadvantage to NuScale.

(b) The information requested to be withheld consists of supporting data, including test data, relative to a process (or component, structure, tool, method, etc.), and the application of the data secures a competitive economic advantage, as described more fully in paragraph 3 of this Affidavit.

(c) Use by a competitor of the information requested to be withheld would reduce the competitor's expenditure of resources, or improve its competitive position, in the design, manufacture, shipment, installation, assurance of quality, or licensing of a similar product.

(d) The information requested to be withheld reveals cost or price information, production capabilities, budget levels, or commercial strategies of NuScale.

(e) The information requested to be withheld consists of patentable ideas.

(3) Public disclosure of the information sought to be withheld is likely to cause substantial harm to NuScale's competitive position and foreclose or reduce the availability of profit-making opportunities. The accompanying report reveals distinguishing aspects about the method by which NuScale develops its NuScale Power Critical Heat Flux Correlation NSP2.

NuScale has performed significant research and evaluation to develop a basis for this method and has invested significant resources, including the expenditure of a considerable sum of money.

The precise financial value of the information is difficult to quantify, but it is a key element of the design basis for a NuScale plant and, therefore, has substantial value to NuScale.

If the information were disclosed to the public, NuScale's competitors would have access to the information without purchasing the right to use it or having been required to undertake a similar expenditure of resources. Such disclosure would constitute a misappropriation of NuScale's intellectual property, and would deprive NuScale of the opportunity to exercise its competitive advantage to seek an adequate return on its investment.

(4) The information sought to be withheld is in the enclosed report entitled "NuScale Power Critical Heat Flux Correlation NSP2".The enclosure contains the designation "Proprietary" at the top of each page containing proprietary information. The information considered by NuScale to be proprietary is identified within double braces, "{{ }}" in the document.

(5) The basis for proposing that the information be withheld is that NuScale treats the information as a trade secret, privileged, or as confidential commercial or financial information. NuScale relies

upon the exemption from disclosure set forth in the Freedom of Information Act ("FOIA"), 5 USC § 552(b)(4), as well as exemptions applicable to the NRC under 10 CFR §§ 2.390(a)(4) and 9.17(a)(4).

(6) Pursuant to the provisions set forth in 10 CFR § 2.390(b)(4), the following is provided for consideration by the Commission in determining whether the information sought to be withheld from public disclosure should be withheld:

(a) The information sought to be withheld is owned and has been held in confidence by NuScale.

(b) The information is of a sort customarily held in confidence by NuScale and, to the best of my knowledge and belief, consistently has been held in confidence by NuScale. The procedure for approval of external release of such information typically requires review by the staff manager, project manager, chief technology officer or other equivalent authority, or the manager of the cognizant marketing function (or his delegate), for technical content, competitive effect, and determination of the accuracy of the proprietary designation. Disclosures outside NuScale are limited to regulatory bodies, customers and potential customers and their agents, suppliers, licensees, and others with a legitimate need for the information, and then only in accordance with appropriate regulatory provisions or contractual agreements to maintain confidentiality.

(c) The information is being transmitted to and received by the NRC in confidence.

(d) No public disclosure of the information has been made, and it is not available in public sources. All disclosures to third parties, including any required transmittals to NRC, have been made, or must be made, pursuant to regulatory provisions or contractual agreements that provide for maintenance of the information in confidence.

(e) Public disclosure of the information is likely to cause substantial harm to the competitive position of NuScale, taking into account the value of the information to NuScale, the amount of effort and money expended by NuScale in developing the information, and the difficulty others would have in acquiring or duplicating the information. The information sought to be withheld is part of NuScale's technology that provides NuScale with a competitive advantage over other firms in the industry. NuScale has invested significant human and financial capital in developing this technology and NuScale believes it would difficult for others to duplicate the technology without access to the information sought to be withheld.

I declare under penalty of perjury that the foregoing is true and correct. Executed on October 5, 2016.

Thomas A. Bergman

Enclosure 4:

AREVA Affidavit

NuScale Power, LLC
1100 NE Circle Blvd., Suite 200 Corvallis, Oregon 97330 Office 541.360-0500 Fax 541.207.3928
www.nuscalepower.com

A F F I D A V I T

COMMONWEALTH OF VIRGINIA)
) ss.
CITY OF LYNCHBURG)

1. My name is Nathan E. Hottle. I am Manager, Product Licensing, for AREVA Inc. (AREVA) and as such I am authorized to execute this Affidavit.

2. I am familiar with the criteria applied by AREVA to determine whether certain AREVA information is proprietary. I am familiar with the policies established by AREVA to ensure the proper application of these criteria.

3. I am familiar with the AREVA information contained in the following document: TR-0116-21012-P, "NuScale Power Critical Heat Flux Correlation NSP2," referred to herein as "Document." Information contained in this Document has been classified by AREVA as proprietary in accordance with the policies established by AREVA Inc. for the control and protection of proprietary and confidential information.

4. This Document contains information of a proprietary and confidential nature and is of the type customarily held in confidence by AREVA and not made available to the public. Based on my experience, I am aware that other companies regard information of the kind contained in this Document as proprietary and confidential.

5. This Document has been made available to the U.S. Nuclear Regulatory Commission in confidence with the request that the information contained in this Document be withheld from public disclosure. The request for withholding of proprietary information is made in accordance with 10 CFR 2.390. The information for which withholding from disclosure is

requested qualifies under 10 CFR 2.390(a)(4) "Trade secrets and commercial or financial information."

6. The following criteria are customarily applied by AREVA to determine whether information should be classified as proprietary:

(a) The information reveals details of AREVA's research and development plans and programs or their results.

(b) Use of the information by a competitor would permit the competitor to significantly reduce its expenditures, in time or resources, to design, produce, or market a similar product or service.

(c) The information includes test data or analytical techniques concerning a process, methodology, or component, the application of which results in a competitive advantage for AREVA.

(d) The information reveals certain distinguishing aspects of a process, methodology, or component, the exclusive use of which provides a competitive advantage for AREVA in product optimization or marketability.

(e) The information is vital to a competitive advantage held by AREVA, would be helpful to competitors to AREVA, and would likely cause substantial harm to the competitive position of AREVA.

The information in this Document is considered proprietary for the reasons set forth in paragraphs 6(c) and 6(d) above.

7. In accordance with AREVA's policies governing the protection and control of information, proprietary information contained in this Document has been made available, on a limited basis, to others outside AREVA only as required and under suitable agreement providing for nondisclosure and limited use of the information.

8. AREVA policy requires that proprietary information be kept in a secured file or area and distributed on a need-to-know basis.

9. The foregoing statements are true and correct to the best of my knowledge, information, and belief.

State of OREGON

County of BENTON

This record was acknowledged before me on SEPTEMBER 21, 2016

by NATHAN HOTTLE.

OFFICIAL STAMP
NATASHA ANDERSON
NOTARY PUBLIC - OREGON
COMMISSION NO. 931120
MY COMMISSION EXPIRES AUGUST 13, 2018

Notary Public – State of Oregon